

VILNIUS UNIVERSITY

Eglė
KUKCINAVIČIŪTĖ

The Response of Chemoresistant Human Colorectal Cancer Cells HCT116 to Cytotoxic Treatment

SUMMARY OF DOCTORAL DISSERTATION

Natural sciences,
Biochemistry N 004

VILNIUS 2019

This dissertation was prepared between 2014 and 2018 at the Institute of Biosciences, Vilnius University. The research was supported by the Research Council of Lithuania (SEN-17/2015).

Academic supervisors:

Prof. Dr. Vida Kirvelienė (Vilnius University, Natural sciences, Biochemistry – N 004). From 2014-10-01 to 2015-09-14.

Doc. Dr. Aušra Sasnauskienė (Vilnius University, Natural sciences, Biochemistry – N 004). From 2015-09-15 to 2018-09-30.

This doctoral dissertation will be defended in a public meeting of the Dissertation Defence Panel:

Chairman – Prof. Dr. Rūta Navakauskienė (Vilnius University, Natural sciences, Biochemistry – N 004).

Members:

Dr. Veronika Borutinskaitė (Vilnius University, Natural sciences, Biochemistry – N 004),

Dr. Augustas Pivoriūnas (State Scientific Research Institute Center for Innovative Medicine, Natural sciences, Biochemistry – N 004),

Dr. Lina Prasmickaitė (Oslo University Hospital, Natural sciences, Biochemistry – N 004),

Prof. Dr. Aurelija Žvirblienė (Vilnius University, Natural sciences, Biochemistry – N 004).

The dissertation shall be defended at a public meeting of the Dissertation Defence Panel at 1 p.m. on 6th of September 2019 in auditorium R101 of the Life Sciences Center, Vilnius University.

Address: Saulėtekio av. 7 – R101, Vilnius, Lithuania

Tel. +37067883581; e-mail: egle.kukcinaviciute@gmail.com

The summary of doctoral thesis was sent on the 6th of August, 2019. The text of this dissertation can be accessed at the library of Vilnius University, as well as on the website of Vilnius University: <https://www.vu.lt/lt/naujienos/ivykiu-kalendorius>

VILNIAUS UNIVERSITETAS

Eglė
KUKCINAVIČIŪTĖ

Chemoterapiniams vaistams
atsparių kolorektalinio vėžio
ląstelių HCT116 atsako į citotoksinį
poveikį molekuliniai aspektai

DAKTARO DISERTACIJOS SANTRAUKA

Gamtos mokslai,
biochemija N 004

VILNIUS 2019

Disertacija rengta 2014 – 2018 metais Vilniaus universitete, Biomokslų institute. Mokslinius tyrimus rėmė Lietuvos mokslo taryba (SEN-17/2015).

Moksliniai vadovai:

prof. dr. Vida Kirvelienė (Vilniaus universitetas, gamtos mokslai, biochemija – N 004). Nuo 2014-10-01 iki 2015-09-14.

doc. dr. Aušra Sasnauskienė (Vilniaus universitetas, gamtos mokslai, biochemija – N 004). Nuo 2015-09-15 iki 2018-09-30.

Gynimo taryba:

Pirmininkė – **prof. dr. Rūta Navakauskienė** (Vilniaus universitetas, gamtos mokslai, biochemija – N 004).

Nariai:

dr. Veronika Borutinskaitė (Vilniaus universitetas, gamtos mokslai, biochemija – N 004),

dr. Augustas Pivoriūnas (Valstybinis mokslinių tyrimų institutas Inovatyvios medicinos centras, gamtos mokslai, biochemija – N 004),

dr. Lina Prasmickaitė (Oslo universiteto ligoninė, gamtos mokslai, biochemija – N 004),

prof. dr. Aurelija Žvirblienė (Vilniaus universitetas, gamtos mokslai, biochemija – N 004).

Disertacija ginama viešame Gynimo tarybos posėdyje 2019 m. rugsėjo mėn. 6 d. 13 val. Vilniaus universiteto Gyvybės mokslų centro R101 auditorijoje. Adresas: Saulėtekio al. 7 – R101, Vilnius, Lietuva. Tel. +37067883581; el. p. egle.kukcinaviciute@gmail.com.

Disertacijos santrauka išsiuntinėta 2019 m. rugpjūčio 6 d.

Disertaciją galima peržiūrėti Vilniaus universiteto bibliotekoje ir VU interneto svetainėje adresu: <https://www.vu.lt/naujienos/ivykiu-kalendorius>

LIST OF ABBREVIATIONS

- 2D model – cells were grown as monolayer
3D model – cells were grown as multicellular spheroids
5-FU – 5-fluorouracil
BSA – bovine serum albumin
CQ – lysosomal acidification inhibitor chloroquine diphosphate
CRC – colorectal cancer
CTB – cell viability assessment using CTB assay
CTT – cytotoxicity
CV – cell viability assessment using crystal violet assay
IC50 value – drug concentration which kills 50% of cells or reduces relative spheroid volume by 50%
LC3B-I – the cytoplasmic form of LC3B protein
LC3B-II – the lipidated form of LC3B protein
mTHPC – 5,10,15,20-tetra(m-hydroxyphenyl)chlorin
MTT – cell viability assessment using MTT assay
NICD1 – NOTCH1 intracellular domain
OxaPt – oxaliplatin
PDT – photodynamic treatment
RO – γ -secretase inhibitor RO4929097
SD – standard deviation
XAV – tankyrase inhibitor XAV939

INTRODUCTION

Colorectal cancer (CRC) is one of most commonly diagnosed cancers not only in Lithuania (9% of new cancer cases, 11% of cancer deaths), but also in the world (9.7% of new cancer cases, 8.5% of cancer deaths) (The Lithuanian Cancer Registry, 2012; Ferlay *et al.*, 2015). Chemotherapy regimen FOLFOX is used for CRC treatment and consists of 5-fluorouracil (5-FU), oxaliplatin (OxaPt) and folinic acid (Cuyle and Prenen, 2017). The primary mechanisms of 5-FU and OxaPt action are different. In cells, 5-FU is converted into its active forms, one of which inhibits thymidylate synthase activity and others induce DNA and RNA strand breaks by direct incorporation into these molecules (Longley *et al.*, 2003). OxaPt undergoes non-enzymatic conversion into highly reactive aqua complexes which form DNA, RNA or protein adducts (Panczyk, 2014; Jensen *et al.*, 2012; Reardon *et al.*, 1999). Chemotherapy response rates for advanced CRC remain low, primarily due to intrinsic or acquired chemoresistance (Dallas *et al.*, 2009; Punt and Tol, 2009).

Non-overlapping treatment regimens could overcome the chemoresistance of cancer cells. One of the regimens could be the photodynamic treatment (PDT). PDT uses light-sensitive compound, a photosensitizer, which is irradiated with visible light. It leads to the generation of ROS which induces tumor cell death. mTHPC (5,10,15,20-tetra(m-hydroxyphenyl)chlorin) is the second-generation photosensitizer and one of the most widely studied drugs in PDT. mTHPC diffusely localizes in cellular organelles (mitochondria, lysosomes, endoplasmic reticulum, Golgi complex) and acts through the generation of singlet oxygen (Chen *et al.*, 2000; Teiten *et al.*, 2003; Marchal *et al.*, 2007; Leung *et al.*, 2002; Senge and Brandt, 2011). It was shown that PDT could be effective in treating chemoresistant cancer cells (Goler-Baron and Assaraf, 2012; Kulbacka *et al.*, 2010; Celli *et al.*, 2011; Yu and Yu, 2014). Some

studies suggest that PDT-based combinations with chemotherapy could re-sensitize chemoresistant cancer cells to standard chemotherapy (Spring *et al.*, 2015).

Multiple mechanisms can cause cellular chemoresistance: alteration of drug metabolism or drug targets, increased cell ability to repair damaged cellular components, activation of pro-survival pathways or defects in cell death pathways (Fodale *et al.*, 2011; Holohan *et al.*, 2013). The cell resistance to chemotherapy-induced stress could also be linked with changes in macroautophagy (hereafter autophagy). During autophagy portions of cytoplasm are sequestered into double-membrane vesicles called autophagosomes and delivered for degradation to lysosomes. Efficient autophagic responses have been associated with the activity of two ubiquitin-like conjugation systems. One relies on ATG7 and ATG10, which promote the conjugation of ATG5 to ATG12 in the context of ATG16L1. Another one is mediated by ATG3 and ATG7, which together with the ATG12-ATG5:ATG16L1 complex conjugates phosphatidylethanolamine to microtubule-associated protein LC3 after ATG4-dependent proteolytic maturation (Galluzzi *et al.*, 2017). Lipidated LC3 (also called LC3-II) is generated onto forming autophagosomes and promotes further growth of isolation membrane. LC3-II allows for substrate uptake upon binding to several autophagy receptors and may be involved in autophagosome closure (Galluzzi *et al.*, 2017; Mercer *et al.*, 2018; Lippai and Szatmari, 2017).

The self-renewal and differentiation of intestinal epithelium are governed by multiple signaling pathways, including Wnt and Notch (van der Flier and Clevers, 2009). The canonical Wnt pathway is activated upon binding of secreted Wnt ligands to Frizzled receptors and LRP5/6 co-receptors which leads to inhibition of destruction complex, thus phosphorylation and degradation of its target – β -catenin is decreased. The accumulation of cytosolic β -catenin leads to translocation of this protein to the nucleus where β -catenin

promotes Wnt transcriptional output (Zhan *et al.*, 2017). Mammalians have four Notch receptors (NOTCH1-4) and five Notch ligands (DLL1,3,4 and JAG1,2) all of which are single-pass transmembrane proteins (Li *et al.*, 2017). Notch signaling is activated by interaction of ligand located on one cell with the receptor present on the neighboring cell, followed by two cleavages, mediated by metalloproteases ADAM10/17 and γ -secretase complex. They lead to the release of Notch receptor intracellular domain (NICD) which translocates to the nucleus and induces the transcription of Notch target genes, which include a strong basic helix–loop–helix (bHLH) transcriptional repressor HES1 (Kopan and Ilagan, 2009). It is important to note that activation of Wnt and Notch signaling pathways are also evident during CRC progression (Pandurangan *et al.*, 2018). That suggests the notion that Wnt and Notch signaling pathways could also be relevant for maintaining cancer cell chemoresistance (Saif and Chu, 2010; Roy and Majumdar, 2012). These signaling pathways depend on cell-to-cell interactions, thus evaluation of their activity in cells grown not only in monolayer but also in spheroid culture is essential.

The objective of the dissertation work was investigate the importance of autophagy and Wnt, Notch signaling pathways for the response of human CRC cells HCT116 and chemoresistant sublines HCT116/FU, HCT116/OXA to 5-FU or OxaPt treatment.

Towards this goal, **the following specific tasks have been formulated:**

- To evaluate the cell survival and extent of autophagy in HCT116 and HCT116/FU cells after mTHPC-PDT and its combinations with 5-FU;
- To compare the extent of autophagy, activation of Wnt/ β -catenin and Notch1 signaling in HCT116/FU, HCT116/OXA cells vs. HCT116 cells after 5-FU or OxaPt treatment;

- To test the importance of Wnt/ β -catenin, Notch signaling and autophagy for HCT116/FU, HCT116/OXA cell resistance to 5-FU or OxaPt.

Scientific novelty

For the first time, we demonstrated that 5-FU-resistant human CRC cells HCT116/FU exhibited higher activation of Wnt/ β -catenin (in the 2D model), Notch1 signaling pathways, elevated HES1 protein levels (both in 2D and 3D models) and higher amount of autophagosomes (in the 2D model) as compared to parental HCT116 cells. Meanwhile 5-FU and OxaPt-resistant HCT116/OXA cells manifested the increase in activation of Wnt/ β -catenin signaling, Notch1 signaling (only in the 2D model), higher HES1 protein levels (in the 2D and 3D models) and lower amount of autophagosomes (in the 2D model) as compared to parental HCT116 cells. The higher activation of Wnt/ β -catenin signaling was reported previously only in 5-FU-resistant CRC cells (Ayadi *et al.*, 2015). Even though higher NOTCH1 protein expression was found in 5-FU or OxaPt-resistant CRC cells (Dinicola *et al.*, 2016; Liu *et al.*, 2016), the activation of this receptor had not been determined.

We were first to evaluate the efficiency of mTHPC-PDT and its combination with 5-FU on sensitive and chemoresistant CRC cells. Even though chemoresistant CRC cells were sensitive to mTHPC-PDT, this treatment was not able to overcome the acquired 5-FU resistance. Our results indicated that mTHPC-PDT blocks autophagic flux in CRC cells. Furthermore, the investigation of autophagy extent after mTHPC-PDT and 5-FU combined treatment revealed that the amount of autophagosomes were more dependent on PDT component, while 5-FU effects on autophagic flux were cell-line dependent.

Our results indicated that 5-FU treatment decreased the HES1 protein levels, weakened the activation of Wnt/ β -catenin and Notch1 signaling pathways in HCT116, HCT116/FU and HCT116/OXA

cells. Even though the inhibition of autophagic flux by 5-FU in HCT116 cells was recorded previously (Liu *et al.*, 2016), we were first to demonstrate that this treatment also downregulated the autophagic flux in chemoresistant CRC cells HCT116/FU, HCT116/OXA. The Wnt/ β -catenin signaling inhibitor XAV enhanced the cytotoxic effects of 5-FU on chemoresistant cells HCT116/FU, HCT116/OXA grown in both 2D and 3D models. While Notch signaling inhibitor RO promoted 5-FU cytotoxicity only on chemoresistant HCT116/FU and HCT116/OXA cells grown in the 3D model. The cytotoxicity of 5-FU was decreased by HES1 protein silencing and was not altered by the reduction of ATG7 protein amount.

We demonstrated that OxaPt treatment reduced Wnt/ β -catenin, Notch1 signaling only in OxaPt-sensitive HCT116 and HCT116/FU cells. Furthermore, this treatment upregulated the autophagic flux in all tested cells. In the 2D model, the inhibitor of Wnt/ β -catenin signaling XAV hindered OxaPt cytotoxicity to HCT116, HCT116/FU, HCT116/OXA cells. While in the 3D model, the effects of this inhibitor on the cytotoxicity of OxaPt were cell-line dependent: in HCT116/FU cells OxaPt cytotoxicity was decreased, in HCT116/OXA cells – increased, in HCT116 cells – not altered. Notch signaling inhibition, HES1 or ATG7 protein silencing reduced OxaPt cytotoxic effect.

Defending statements

- mTHPC-PDT was cytotoxic to HCT116/FU cells but did not overcome their acquired resistance to 5-FU.
- In the chemoresistant cells HCT116/FU (resistant to 5-FU) and HCT116/OXA (resistant to 5-FU and OxaPt), the activation of Wnt/ β -catenin and Notch1 signaling is increased.
- The Wnt/ β -catenin and Notch signaling affected the survival or death of cells after 5-FU or OxaPt treatments, while the autophagy promoted cell death after OxaPt treatment.

Doctoral thesis contents

The doctoral thesis (in Lithuanian) contains the following parts: Introduction, Literature overview, Material and Methods, Results, Discussion, Conclusions, Supplements (2), List of references (424 citations), List of publications (2 positions), Participation at conferences (4 positions), Figures (23), Tables (15). Total number of pages – 113.

1. Materials and Methods

Cell lines. Human colorectal carcinoma cells HCT116 were purchased from the ATCC. Chemoresistant subline HCT116/FU was generated by continuously culturing HCT116 cells in a medium containing 5-FU (drug concentration increased from 10 μ M until 100 μ M) for 1 year until the cells acquired stable resistance. HCT116/OXA subline was generated by continuously culturing HCT116 cells in a medium containing OxaPt (drug concentration increased from 1 μ M until 20 μ M) for 9 months until the cells acquired stable resistance. All cell lines were cultured in RPMI 1640 medium supplemented with 10% fetal bovine serum, 2 mM L-glutamine and 0.05 mg/mL gentamycin in a humidified atmosphere at 37°C in 5% CO₂.

Drugs and chemicals. Anticancer drugs 5-FU (50 mg/mL, Accord Healthcare) and OxaPt (5 mg/mL, Accord Healthcare) were used for the study. Photosensitizer mTHPC was dissolved in ethanol and stored at -20°C in the dark. γ -secretase inhibitor RO4929097 (RO, Selleckchem) and tankyrase inhibitor XAV939 (XAV, Selleckchem) were dissolved in DMSO and stored at -20°C or -70 C. Lysosomal acidification inhibitor chloroquine diphosphate (CQ, Sigma) was dissolved in ddH₂O and stored at -20°C. Stock solutions of drugs and inhibitors were diluted in growth medium at appropriate concentrations just before the use.

Monolayer cell culture. For the evaluation of cells response to 5-FU or OxaPt treatment, cells were seeded at the density of 1×10^5 cells/mL (HCT116), 1.5×10^5 cells/mL (HCT116/OXA) or 2×10^5 cells/mL (HCT116/FU), which gives the same cells confluence at the time of adding the drug. If indicated, cells were treated with: 5-FU (0.03 – 3 mM) or OxaPt (0.01 – 0.6 mM) at 48 h after seeding; XAV (15 μ M) or RO (5 μ M) at 24 h after seeding; CQ (30 μ M) at 4 h prior to sample collection for Western blotting. Cells were harvested for Western blotting and cell viability was

determined at 48 h post exposure to anticancer drugs using crystal violet or MTT assay (Fig. 1.1).

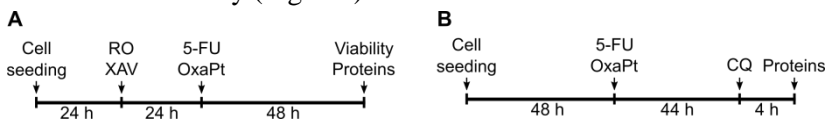


Fig. 1.1 Schedule for cell treatment with 5-FU or OxaPt. A, Schedule for cell treatment when the activation of Wnt or Notch signaling was evaluated. B, Schedule for cell treatment when the effect of drugs on autophagy-related proteins was tested. The doses of inhibitors: 15 μ M XAV, 5 μ M RO, 30 μ M CQ.

For the evaluation of cells response to mTHPC, cells were seeded at the density of 1.5×10^5 cells/mL (HCT116) or 3.0×10^5 cells/mL (HCT116/FU). After 48 h, cell medium was replaced with serum-free medium containing 0.1 μ g/mL mTHPC and/or 5-FU (0.01 – 10 mM) and cells were further incubated in the reduced light environment for 18 h. Photodynamic treatment was induced by exposing cells to light for 30 – 270 s from LED array UNIMELA-1 ($\lambda=660\pm 5$ nm; 10 mW/cm²). Cells were harvested for Western blotting and cell viability was determined at 48 h post exposure to anticancer drugs using crystal violet assay. If indicated cells were treated with 30 μ M CQ at 4 h prior to sample collection for Western blotting (Fig. 1.2).

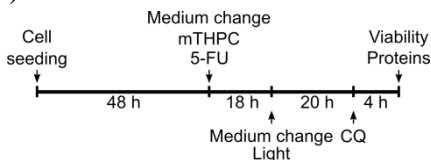


Fig. 1.2 Schedule for cell treatment with mTHPC and/or 5-FU. The dose of inhibitor: 30 μ M CQ. Light, cell exposure to light using LED array UNIMELA-1 ($\lambda=660\pm 5$ nm; 10 mW/cm²).

Spheroid cell culture. HCT116, HCT116/FU, HCT116/OXA cells were seeded on flat bottom 96-well cell culture plates coated with 1.4% agarose solution in RPMI 1640 medium (prepared as described in (Friedrich *et al.*, 2009)) at the density of 750, 950 and 850 cells/well, respectively. At 96 h after initiation, each well was imaged with Nikon ECLIPSE TS100 microscope equipped with

Lumenera's INFINITY1-1M camera. Images were analyzed with SpheroidSizer software (Chen *et al.*, 2014) and only spherical-shaped spheroids with the volume of $0.0210 \pm 0.0012 \text{ mm}^3$ were selected for the experiments (Zanoni *et al.*, 2016). If indicated spheroids were treated with the drug (1 – 30 μM 5-FU or 0.6 – 30 μM OxaPt) and/or inhibitor (1 μM RO; 1 μM XAV) at 96 h after initiation. For evaluation of drug cytotoxicity, half of the medium in each well was replaced with the fresh one at 72 h after exposure to drug and relative spheroid volume was determined at 120 h after exposure to drug (relative spheroid volume – the ratio between the volume of drug-treated spheroid and the volume of untreated spheroid $\times 100\%$). Spheroids were collected for Western blotting at 72 h after exposure to drugs (Fig. 1.3).

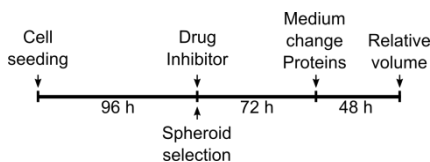


Fig. 1.3 Schedule for spheroid treatment with 5-FU or OxaPt. The doses of inhibitors: 1 μM XAV, 1 μM RO.

siRNA transfection. A small interfering siRNAs targeted to HES1 (HES1 siRNA, 5'-ccacgugcgagggcguuaatt-3'), ATG7 (ATG7 siRNA, 5'-ggagucacagcucuuccuuuutt-3') and the negative control, which had a sequence with no homology to any human mRNA (NT siRNA, 5'-agguaguguaaucgccuuguutt-3'), were used. Cells were seeded in growth medium without antibiotics at different densities (Table 1.1). After 24 h, transfection mixtures were prepared using Lipofectamine® RNAiMAX (Thermo Fisher Scientific) transfection reagent and Opti-MEM (Thermo Fisher Scientific) medium:

- for HES1 siRNA transfection: 3.6 pmol siRNA (diluted in 20 μL Opti-MEM) mixed with 0.6 μL Lipofectamine® RNAiMAX (diluted in 20 μL Opti-MEM), incubated for 15 min at room temperature and added to the well which has 0.9 cm^2 growth area.

- for ATG7 siRNA transfection: 0.5 pmol siRNA (diluted in 5 μ L Opti-MEM) mixed with 0.15 μ L Lipofectamine® RNAiMAX (diluted in 5 μ L Opti-MEM), incubated for 15 min at room temperature and added to the well which has 0.32 cm² growth area.

At 24 h after transfection, the medium was replaced and cells treated with 5-FU (0.1mM or 1mM) or OxaPt (0.03mM or 0.3mM). Cell viability was assessed at 48 h post exposure to anticancer drugs using MTT or CTB assay.

Table 1.1 The cell seeding densities for siRNA transfection.

| Cell line | Cell seeding density for the well which has growth area of | |
|------------|--|----------------------|
| | 0.75 – 3.8 cm ² | 0.32 cm ² |
| HCT116 | 1,5×10 ⁵ cells/mL | 3000 cells/well |
| HCT116/FU | 2,5×10 ⁵ cells/mL | 6000 cells/well |
| HCT116/OXA | 2,0×10 ⁵ cells/mL | 4500 cells/cell |

Crystal violet (CV) assay. The cells were washed with PBS or 0.9% NaCl, fixed with 96% ethanol for 10 min, stained with 0.05% crystal violet solution in 20% ethanol for 30 min. After that the cells were rinsed, the remaining cell-attached dye was dissolved in 0.1% acetic acid solution in 50% ethanol and the absorbance was recorded at 585 nm using spectrophotometer Asys UVM340.

MTT assay. The cells were washed with DPBS and incubated with 0.1 mg/mL MTT (Sigma) solution in DPBS for 1 h at +37°C. The water-insoluble MTT reduction product (produced by viable cells) was dissolved in isopropanol and the absorbance was recorded at 570 nm using spectrophotometer Asys UVM340.

CTB assay. To each 100 μ L of cell medium, 20 μ L of CellTiter-Blue® (CTB, Promega) reagent was added and cells were incubated for 1 h at +37°C. The fluorescence of CTB reduction product (produced by viable cells) was measured using spectrofluorometer Varioskan Flash ($\lambda_{ex.}$ =560 nm, $\lambda_{em.}$ =590 nm).

Western blotting. Substratum-bound and detached cells (for experiments in monolayer cell culture) or at least 30 spheroids (for

every experimental condition in spheroid cell culture) were collected and lysed for 30 min on ice in RIPA buffer (100 μ L buffer for 1×10^6 cells or 45 spheroids): 50 mM Tris-HCl (pH 7.4), 150 mM NaCl, 1 mM EDTA, 1% Triton X-100, 1% sodium deoxycholate, 0.1% sodium dodecyl sulfate and appropriate amount of Protease Inhibitor Cocktail for General Use (Sigma). Then cell lysates were centrifuged for 5 min at $14\,000 \times g$ and 4°C . The supernatant was collected and protein concentration was determined by BCA method. Protein samples were subjected to 12% SDS-PAGE at 120 V, then transferred to nitrocellulose membrane (BioRad) by semi-dry blotting. Blots were probed with anti-ATG7 antibody (MAB6608, R&D Systems), anti-LC3B antibody (ab51520, Abcam), anti-NICD1 antibody (4147S, Cell Signalling), anti-HES1 antibody (PA5-28802, Thermo Scientific) or the anti-non-phospho β -catenin antibody (8814S, Cell Signalling). In addition, the blots were probed with anti- β -actin antibody (MA5-15739, Thermo Scientific) for detection of β -actin as a loading control. Membrane-bound primary antibodies of LC3B, NICD1, HES1, β -catenin were detected by the horseradish-peroxidase-conjugated secondary anti-rabbit antibody (31460, Thermo Scientific). The antibodies of ATG7 and β -actin were detected by the horseradish-peroxidase-conjugated secondary anti-mouse antibody (31430, Thermo Scientific). The immunoreactive bands were developed using Pierce® ECL Western Blotting Substrate (Thermo Scientific).

Immunofluorescence. The cells were seeded in 96-well plate (Ibidi) at the densities of: for control samples – 1500 (HCT116) or 2000 cells/well (HCT116/FU, HCT116/OXA); for samples treated with drugs – 3000 (HCT116, HCT116/OXA) or 4000 cells/well (HCT116/FU). Cells were treated with 5-FU or OxaPt (at 48 h post seeding), CQ (at 4 h prior to cell fixation) and fixed (at 48 h post drug addition) with ice-cold methanol. After blocking with 3% BSA in PBS, cells were incubated with anti-LC3B antibody (ab51520, Abcam) and labeled with goat anti-rabbit IgG secondary antibody

which is conjugated with Alexa Fluor® 647 (A21244, Invitrogen). Immunofluorescence was registered with $\lambda_{\text{ex.}}=604 - 644 \text{ nm}$, $\lambda_{\text{em.}}=672 - 712 \text{ nm}$.

Statistical analysis. SigmaPlot 12.5 software was used for statistical analysis. Data are presented as mean \pm SD from three independent assays, each one at least in triplicate. For the determination of relative spheroid volume, each dose of the drug was tested on at least six spheroids. Regression analysis was performed for the evaluation of IC_{50} values. The effect of combined treatment on cell viability was evaluated by the two-way ANOVA. The Mann–Whitney U test or two-sample t-test was used to compare differences between two independent groups. Significance was accepted with the P-value <0.05 .

2. Results

2.1 The cytotoxicity of 5-FU, OxaPt or mTHPC-PDT

2.1.1 The cytotoxicity of 5-FU or OxaPt

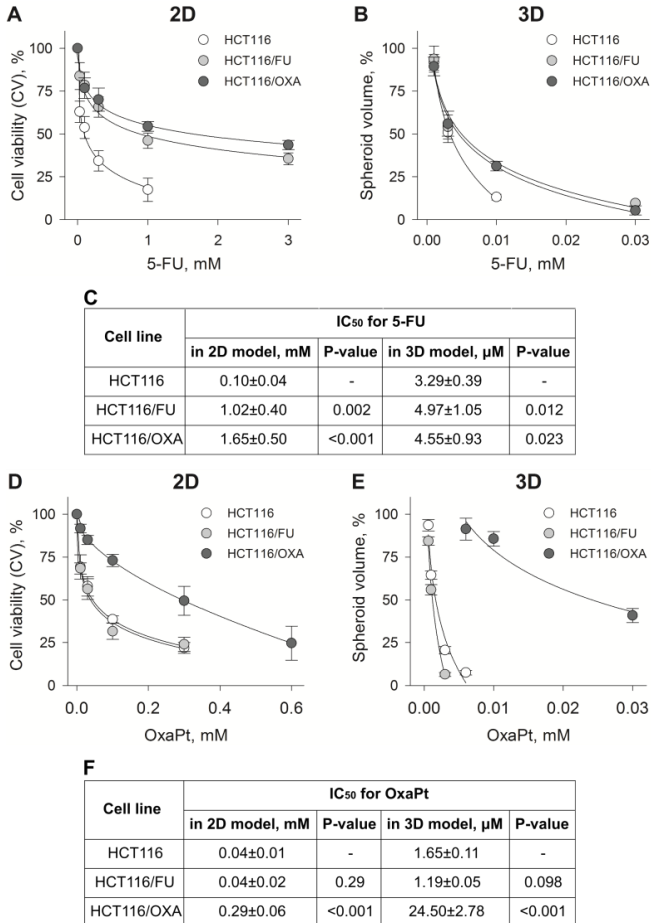


Fig 2.1 The cytotoxicity of 5-FU and OxaPt to HCT116, HCT116/FU and HCT116/OXA cells. Cell viability (A) and relative spheroid volume (B) after treatment with 5-FU. C, IC₅₀ values for 5-FU in the 2D and 3D models. Cell viability (D) and relative spheroid volume (E) after treatment with OxaPt. C, IC₅₀ values for OxaPt in the 2D and 3D models. Cell viability was determined at 48 h after drug addition using CV assay. Relative spheroid volume was determined at 120 h after adding the drug. n≥3; Error bars ± SD.

The sensitivity of HCT116, HCT116/FU and HCT116/OXA cells grown in monolayer and spheroid culture to single 5-FU or OxaPt treatment have been tested (Fig. 2.1). The regression analysis of exponential dose-response curves was performed in order to determine the drug concentrations which kill 50% of cells or reduce the relative spheroid volume by 50% (IC₅₀ values) (Fig. 2.1 C, F). After the comparison of these values we assessed that HCT116/FU cells acquired significant chemoresistance to 5-FU treatment: in the 2D model HCT116/FU cells were for 10.2 folds (P=0.002) and in the 3D model for 1.5 folds (P=0.012) more resistant to 5-FU when compared to HCT116 cells/spheroids. No significant chemoresistance to OxaPt treatment was evident in HCT116/FU cells either in the 2D model (P=0.290) or 3D model (P=0.098). Moreover, HCT116/OXA cells/spheroids were more resistant than HCT116 cells/spheroids to both 5-FU and OxaPt treatment: the resistance to 5-FU treatment was increased for 16.5 folds in the 2D model (P<0.001) and for 1.4 folds in the 3D model (P=0.023); the resistance to OxaPt treatment was increased for 7.25 folds in the 2D model (P<0.001) and 14.8 folds in the 3D model (P<0.001).

2.1.2 The photocytotoxicity of mTHPC

Significant cytotoxic effect of mTHPC-PDT on HCT116 and HCT116/FU cells was recorded, and the cytotoxicity of PDT increased with increasing duration of light exposure (Fig. 2.2 A, no 5-FU). The evaluation of the combined treatment with 5-FU and mTHPC-PDT by the two-way ANOVA revealed that in HCT116 cells, both the concentration of 5-FU and the duration of light exposure in the presence of mTHPC were significant determinants (P<0.001) of cytotoxic effect (Table 2.1). However, in HCT116/FU cells, the duration of light exposure in the presence of mTHPC was a significant determinant (P<0.001) of the cytotoxic effect, while the

added value of 5-FU in the combination was not significant (P=0.282).

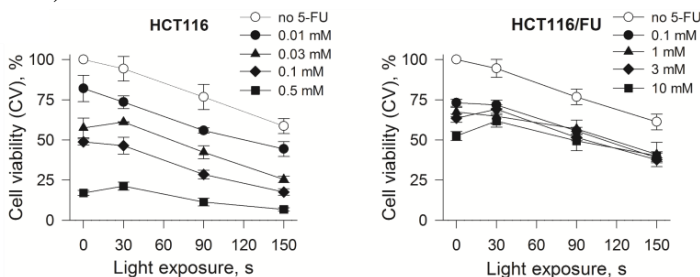


Fig. 2.2 The photocytotoxicity of mTHPC combination with 5-FU on HCT116 and HCT116/FU cells. PDT was induced by incubation of cells with 0.1 $\mu\text{g}/\text{mL}$ mTHPC for 18 h which was followed by exposure to light from LED array UNIMELA-1 ($\lambda=660\pm 5$ nm, 10 mW/cm^2). Cell viability was determined at 24 h post exposure to light using CV assay. $n\geq 3$; Error bars \pm SD.

Table 2.1. The significance of the cytotoxic effect of treatment factors

| Treatment | Cells | HCT116 | | HCT116/FU | |
|------------|-------|------------------------------------|-----------------|------------------------------------|-----------------|
| | | <i>F</i> statistic _(df) | <i>P</i> -value | <i>F</i> statistic _(df) | <i>P</i> -value |
| PDT | | 162 _(2, 12) | <0.001 | 106 _(2, 18) | <0.001 |
| 5-FU | | 77 _(3, 12) | <0.001 | 1 _(2, 18) | 0.282 |
| 5-FU + PDT | | 1 _(6, 12) | 0.623 | 2 _(4, 18) | 0.115 |

df, degrees of freedom

2.1.3 Doses of treatment

For the evaluation of 5-FU and OxaPt effect on Wnt signaling, Notch signaling and autophagy, two doses of 5-FU (0.1 mM and 0.3 mM) or OxaPt (0.03 mM and 0.06 mM) were used, reducing cell viability as shown in Table 2.2.

Table 2.2. The doses of drugs used for Wnt and Notch activation or autophagy measurements and their cytotoxicities (CTT)

| Cell line | 5-FU, mM | | OxaPt, mM | |
|------------|----------|-------|-----------|-------|
| | 0.1 | 0.3 | 0.03 | 0.06 |
| HCT116 | CTT50 | CTT70 | CTT50 | CTT70 |
| HCT116/FU | CTT20 | CTT30 | CTT50 | CTT70 |
| HCT116/OXA | CTT20 | CTT30 | CTT10 | CTT20 |

2.2 Autophagy

The extent of autophagy was evaluated by measuring the protein amounts of the lipidated form of LC3B (LC3B-II) which correlates with the number of autophagosomes (Mizushima and Yoshimori, 2007). In order to assess the autophagic flux, the degradation of autophagosomes was inhibited by lysosomal pH neutralizing agent chloroquine diphosphate (CQ) and the amounts of LC3B-II in the presence and the absence of lysosomal degradation were compared (Klionsky *et al.*, 2016). The amounts of ATG7 protein, which is needed for LC3/GABARAP protein lipidation, were also determined (Nakatogawa, 2013; Antonioli *et al.*, 2017).

2.2.1 The effects of 5-FU or OxaPt on autophagy

The untreated chemoresistant HCT116/FU cells had 1.5 folds higher ($P<0.001$), while HCT116/OXA cells had 1.5 folds lower ($P=0.007$) amounts of LC3B-II protein than HCT116 cells (Fig. 2.3 A). The inhibition of autophagosomes degradation by 30 μM CQ revealed the significant autophagic flux: CQ increased the amounts of LC3B-II protein for 1.5 folds in HCT116 cells ($P<0.001$), for 1.3 folds in HCT116/FU cells ($P<0.001$) and for 1.4 folds in HCT116/OXA cells ($P=0.036$). The significant autophagic flux was also confirmed by immunofluorescence microscopy (Fig. 2.3 B, Control): without CQ, the most of LC3B protein was diffusely distributed in cells, while after CQ treatment, intense punctate LC3B structures (autophagosomes) were evident.

The 5-FU effects on the amounts of autophagosomes were cell-line dependent (Fig. 2.3 A). Only 0.1 mM 5-FU reduced these amounts in HCT116 cells (for 1.3 folds; $P<0.001$). Both 5-FU doses reduced them in HCT116/FU cells (0.1 mM – for 1.3 folds, $P<0.001$; 0.3 mM – for 1.6 folds, $P<0.001$). While in HCT116/OXA cells both 5-FU doses increased them: only slight increase was evident after

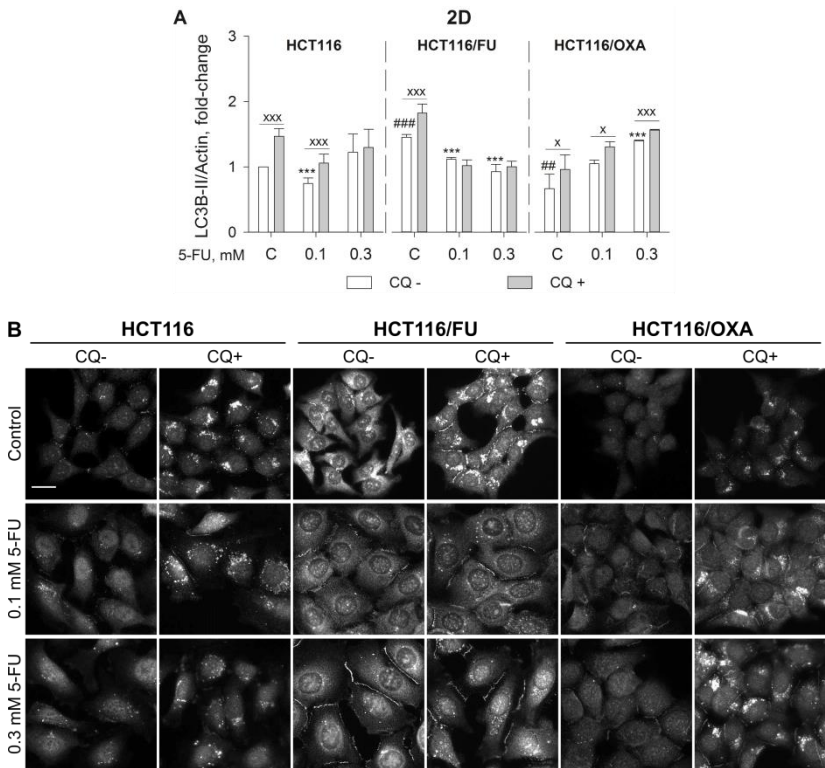


Fig. 2.3 The effects of 5-FU on LC3B protein levels. A, Western blot analysis of LC3B-II (the phosphatidylethanolamine conjugated form) at 48 h after exposure to 5-FU in monolayer cell culture (2D model). B, immunofluorescence analysis of LC3B at 48 h after exposure to 5-FU. The degradation of autophagosomes was inhibited by treatment with 30 μ M CQ at 4 h prior to protein extraction/immunofluorescence analysis. Scale bar – 20 μ m; C, untreated cells; $n \geq 3$; Error bars \pm SD.

#, a statistically significant difference between HCT116/FU or HCT116/OXA vs. HCT116 cells;

*, a statistically significant difference between treated vs. control cells;

x, a statistically significant difference between CQ treated vs. CQ untreated cells.

x/* $p < 0.05$; xx/###/** $p \leq 0.01$; xxx/####/*** $p \leq 0.001$.

0.1 mM 5-FU ($P=0.056$) and after 0.3 mM 5-FU treatment these amounts were upregulated for 2.1 folds ($P < 0.001$). The 5-FU treatment also distressed the autophagic flux: in HCT116/FU cells it was fully inhibited by both 5-FU doses (as seen both in Fig. 2.3 A

and B), in HCT116 cells – inhibited by 0.3 mM 5-FU, in HCT116/OXA cells – reduced for 1.15 folds by 0.1 mM (P=0.048) and for 1.3 folds by 0.3 mM (P=0.001) as compared to the autophagic flux observed in control HCT116/OXA cells.

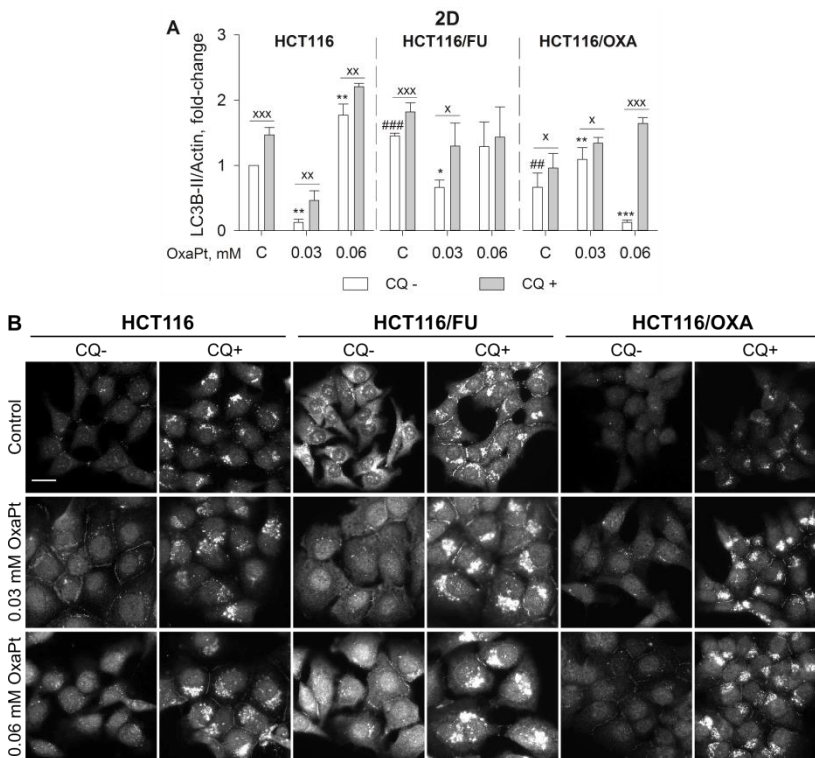


Fig. 2.4 The effects of OxaPt on LC3B protein levels. A, Western blot analysis of LC3B-II (the phosphatidylethanolamine conjugated form) at 48 h after exposure to OxaPt in monolayer cell culture (2D model). B, immunofluorescence analysis of LC3B at 48 h after exposure to OxaPt. The degradation of autophagosomes was inhibited by treatment with 30 μ M CQ at 4 h prior to protein extraction/immunofluorescence analysis. Scale bar – 20 μ m; C, untreated cells; n \geq 3; Error bars \pm SD.

#, a statistically significant difference between HCT116/FU or HCT116/OXA vs. HCT116 cells;

*, a statistically significant difference between treated vs. control cells;

x, a statistically significant difference between CQ treated vs. CQ untreated cells.

x/* p<0.05; xx/##/** p \leq 0.01; xxx/###/**** p \leq 0.001.

0.03 mM OxaPt decreased the amounts of LC3B-II in HCT116 (for 7.9 folds, $P<0.001$) and HCT116/FU cells (for 2.2 folds, $P=0.016$) (Fig. 2.4 A). It had an opposite effect on these levels in HCT116/OXA cells – they were increased for 1.6 folds ($P=0.01$). The autophagic flux was increased for 2.5 folds in HCT116 ($P=0.005$), for 1.6 folds in HCT116/FU cells ($P=0.035$) and decreased for 1.2 folds in HCT116/OXA cells ($P=0.047$) as compared to the autophagic flux observed in cells which were not treated with the drug. Similar trends were revealed by immunofluorescence microscopy (Fig. 2.4 B, 0.03 mM OxaPt treatment), where this treatment had not abolished autophagic flux.

The action of 0.06 mM OxaPt treatment on the autophagy was cell line-dependent. In HCT116 cells, the amounts of autophagosomes were increased for 1.8 folds ($P=0.008$), while the autophagic flux decreased for 1.2 folds ($P=0.009$). The opposite was seen in HCT116/OXA cells, where the amounts of autophagosomes were decreased for 5.2 folds ($P<0.001$) and autophagic flux increased for 8.8 folds. Meanwhile, in HCT116/FU cells, 0.06 mM OxaPt had no effect on autophagosome amounts and significant autophagic flux was only evident in immunofluorescence microscopy (2.4 pav. B, 0.06 mM OxaPt).

The level of ATG7 protein in untreated chemoresistant HCT116/FU cells was 1.2 folds higher ($P<0.001$) and in HCT116/OXA cells – 1.4 folds higher ($P<0.001$) than in HCT116 cells (Fig. 2.5 A). All tested 5-FU and OxaPt doses decreased ATG7 levels in HCT116 cells: these levels were reduced for 39% by 0.1 mM ($P<0.001$) and for 67% by 0.3 mM 5-FU ($P<0.001$), for 43% by 0.03 mM ($P<0.001$) and for 74% by 0.06 mM OxaPt ($P<0.001$). In HCT116/FU cells, these treatments had slightly weaker effect: 0.1 mM 5-FU reduced ATG7 protein levels for 9% ($P=0.016$), 0.3 mM 5-FU – for 37% ($P<0.001$), 0.03 mM OxaPt – for 33% ($P=0.001$) and 0.06 mM OxaPt – for 31% ($P<0.001$). Only 0.3 mM 5-FU decreased ATG7 protein levels in HCT116/OXA cells (for

33%, $P=0.005$), while both OxaPt doses increased them (0.03 mM – for 23%, $P=0.008$; 0.06 mM – for 29%, $P<0.001$).

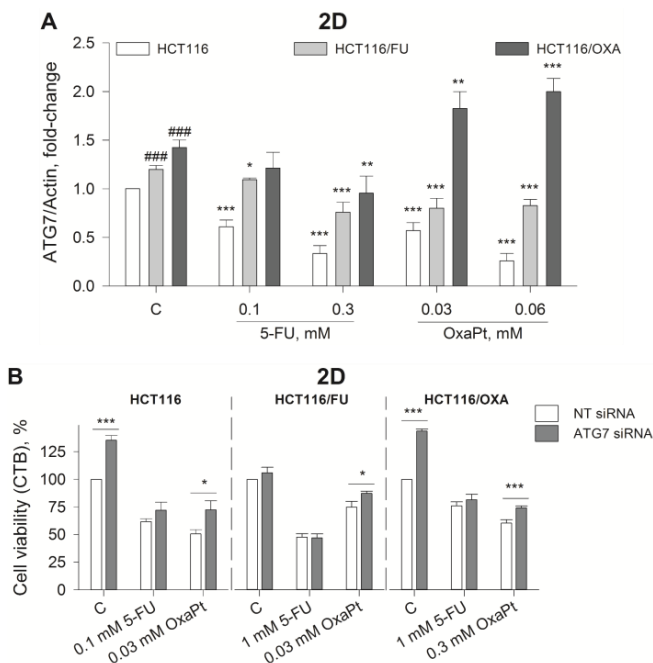


Fig. 2.5 ATG7 level and effects of its silencing on 5-FU and OxaPt cytotoxicity.

A, Western blot analysis of ATG7 at 48 h after exposure to drugs in monolayer cell culture (2D model). B, the effects of ATG7 silencing on 5-FU and OxaPt cytotoxicity. ATG7 was downregulated by transfection of ATG7 targeting siRNA at 24 h prior to exposure to drugs. Cell viability was determined at 48 h after exposure to drugs using CTB assay. C, untreated cells; $n \geq 3$; Error bars \pm SD.

#, a statistically significant difference between HCT116/FU or HCT116/OXA vs. HCT116 cells;

*, a statistically significant difference between treated vs. control cells.

* $p < 0.05$; ##/** $p \leq 0.01$; ###/*** $p \leq 0.001$.

The expression of ATG7 was downregulated using siRNA, to explore the significance of this protein for the cytotoxic effects of 5-FU and OxaPt. At 48 h post siRNA transfection, the reduction of ATG7 protein levels in all cell lines was approx. 75% (data not shown). The downregulation of ATG7 increased the viability of HCT116 (for 35%, $P < 0.001$) and HCT116/OXA cells (for 40%,

$P < 0.001$). The cells sensitivity to 5-FU treatment was not affected by ATG7-silencing, while sensitivity to OxaPt treatment was reduced: 0.03 mM OxaPt dose was 23% less cytotoxic on HCT116 cells ($P = 0.026$) and 12% less cytotoxic on HCT116/FU cells ($P = 0.038$); 0.3 mM OxaPt was 14% less cytotoxic on HCT116/OXA cells ($P = 0.004$).

2.2.2 The effects of mTHPC-PDT on autophagy

mTHPC-PDT used as a single treatment, upregulated the levels of LC3B-II protein in both cell lines, except for 90s PDT in the HCT116/FU cells (Fig. 2.6 A): in HCT116 cells these levels increased for 4.5 folds after 90s PDT ($P = 0.006$), for 10.8 folds after 180s PDT ($P < 0.001$) and for 10.5 folds after 270s PDT ($P < 0.001$); in HCT116/FU cells – for 10.8 folds after 180s PDT ($P < 0.001$) and for 11.1 folds after 270s PDT ($P < 0.001$). However, the degradation of autophagosomes was disrupted by this treatment – autophagic flux was inhibited by all doses of light exposure, except for 90s PDT in HCT116/FU cells where autophagic flux was 1.6 folds higher than in untreated cells ($P = 0.006$).

The combination of mTHPC-PDT with 5-FU affected autophagy in HCT116 and HCT116/FU cells (Fig. 2.6 B). In HCT116 cells, the addition of 5-FU had the negative effect on LC3B-II protein levels induced by 90s PDT: 0.03 mM 5-FU reduced these levels for 2.4 folds ($P = 0.016$), 0.1 mM 5-FU – for 3.3 folds ($P = 0.009$). However, 5-FU promoted autophagic flux – the combination of 90s PDT with 0.03 mM, 0.1 mM or 0.3 mM 5-FU resulted in higher autophagic flux as compared to single 90s PDT: 0.03 mM increased it for 2 folds ($P < 0.001$), 0.1 mM – for 3.8 folds ($P < 0.001$), 0.3 mM – for 2.2 folds ($P < 0.001$). Meanwhile in HCT116/FU cells (as compared to single 90s PDT), the addition of 5-FU had the positive effect on LC3B-II protein levels, but decreased autophagic flux: 1 mM 5-FU addition resulted in a 1.9 fold increase of LC3B-II levels ($P = 0.021$) and autophagic flux inhibition; 3 mM 5-FU – in 1.9 fold

decrease of LC3B-II levels ($P=0.004$) and 1.9 fold decrease in autophagic flux ($P=0.006$); 10 mM 5-FU – in 9 folds increase of LC3B-II levels ($P<0.001$) and inhibition of the autophagic flux.

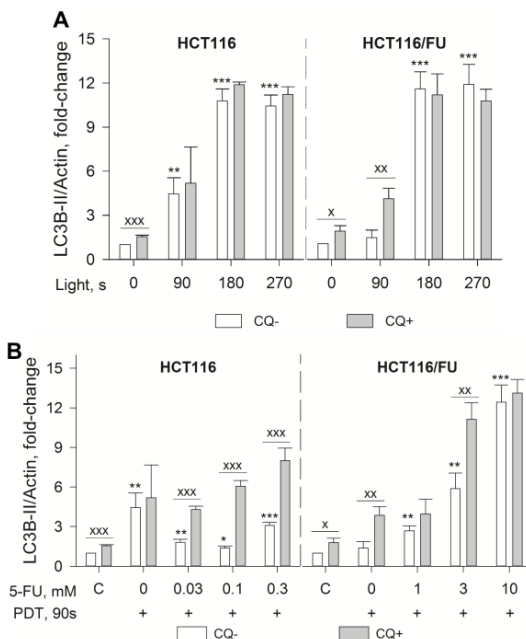


Fig. 2.6 The effects of mTHPC-PDT combination with 5-FU on autophagy in HCT116 and HCT116/FU cells. The dependence of LC3B-II levels on the duration of light exposure (A) and the combinations of PDT with different 5-FU doses (B) at 24 h post exposure to light. PDT was induced by incubation of cells with 0.1 $\mu\text{g}/\text{mL}$ mTHPC for 18 h which was followed by exposure to light from LED array UNIMELA-1 ($\lambda=660\pm 5$ nm, 10 mW/cm^2). The degradation of autophagosomes was inhibited by treatment with 30 μM CQ at 4 h prior to protein extraction. C, untreated cells; $n\geq 3$; Error bars \pm SD.

*, a statistically significant difference between treated vs. control cells;
 x, a statistically significant difference between CQ treated vs. CQ untreated cells.
 x/* $p<0.05$; xx/** $p\leq 0.01$; xxx/*** $p\leq 0.001$.

2.3 Wnt/ β -catenin signaling

The activation of canonical Wnt signaling was evaluated by measuring the levels of non-phosphorylated β -catenin at residues Ser33, Ser37, and Thr41 (the active form of β -catenin). In the 2D cell

culture, the untreated HCT116/FU and HCT116/OXA cells had approx. 1.5 folds higher amounts of active β -catenin than HCT116 cells ($P<0.001$ and $P=0.004$, respectively). Moreover, in the 3D cell culture the increase in this protein levels in untreated chemoresistant spheroids was also significant – in HCT116/FU spheroids the levels were 1.2 folds higher ($P=0.018$) and in HCT116/OXA spheroids – 1.3 folds higher ($P<0.001$) than in untreated HCT116 spheroids (Fig. 2.7 A).

The level of active β -catenin in HCT116 cells grown in 2D cell culture was only affected by high dose of 5-FU and OxaPt: 0.3 mM 5-FU treatment reduced this level for 36% ($P<0.001$) and 0.06 mM OxaPt reduced it for 49% ($P<0.001$). Both doses of 5-FU and high dose of OxaPt reduced β -catenin level in HCT116/FU cells: 0.1 mM 5-FU for 44% ($P=0.002$), 0.3 mM 5-FU for 27% ($P=0.012$), 0.06 mM OxaPt for 57% ($p=0.001$). Only 5-FU, but not OxaPt treatment, had a significant effect on the active β -catenin level in HCT116/OXA cells: it was reduced for 35% by 0.1 mM 5-FU ($P=0.017$) and for 53% by 0.3 mM 5-FU ($P=0.005$).

The importance of Wnt/ β -catenin signaling for the cytotoxic effects of 5-FU and OxaPt was studied using inhibitor XAV939 (XAV). It inhibits the tankyrases, thus promoting Axin stabilization and β -catenin degradation (Huang *et al.*, 2009). When used as a single treatment 15 μ M XAV did not affect cell viability in the 2D cell culture (Fig. 2.7 B, D). However, 1 μ M XAV was toxic for chemoresistant HCT116/FU and HCT116/OXA spheroids: it reduced the relative volumes of HCT116/FU and HCT116/OXA spheroids by 24% ($P<0.001$) and 11% ($P=0.012$), respectively (Fig. 2.7 C, E).

In the 2D cell culture, the cytotoxic effect of 0.1 mM 5-FU was enhanced by the addition of 15 μ M XAV: the viability decreased by 9% in HCT116 cells ($P=0.003$), by 15% in HCT116/FU cells ($P=0.008$) and by 30% in HCT116/OXA cells ($P=0.001$) as compared to single 5-FU treatment (Fig. 2.7 B). Whereas in the 3D

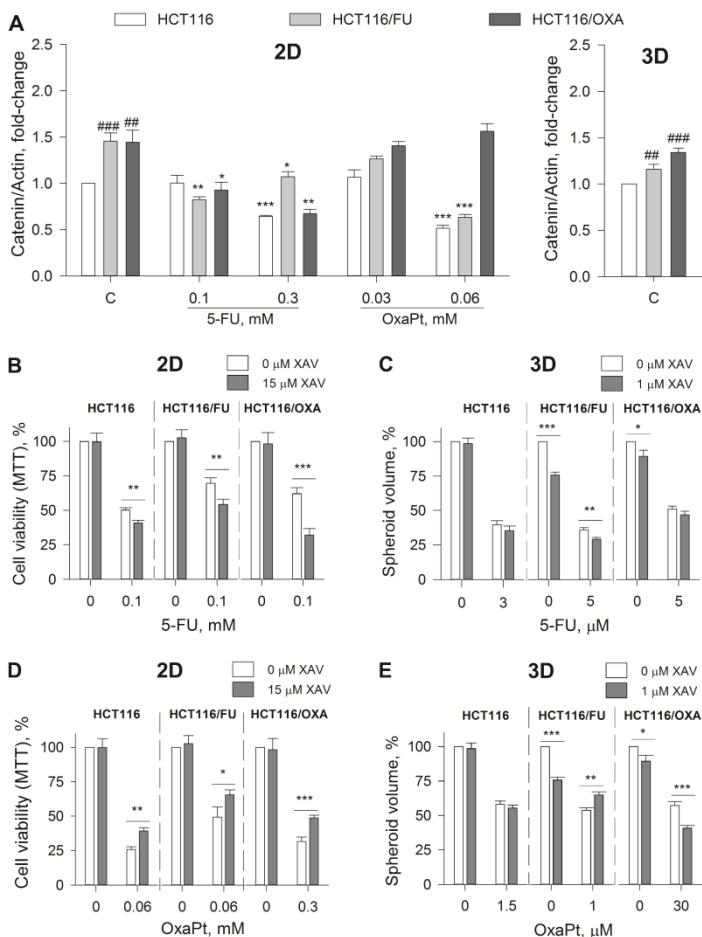


Fig. 2.7 The effects of 5-FU and OxaPt on Wnt signaling. A, Western blot analysis of the active form of β -catenin at 48 h after exposure to drugs in monolayer cell culture (2D model) and in control spheroids at 168 h after initiation (3D model). The effects of XAV on 5-FU cytotoxicity in the 2D (B) and 3D (C) cell culture. The effects of XAV on OxaPt cytotoxicity in the 2D (D) and 3D (E) cell culture. Cell viability was determined at 48 h after exposure to drugs using MTT assay. Relative spheroid volume was determined at 120 h after drug addition. C, untreated cells; n=3; Error bars \pm SD.

#, a statistically significant difference between HCT116/FU or HCT116/OXA vs. HCT116 cells;

*, a statistically significant difference between treated vs. control cells.

* $p < 0.05$; ##/** $p \leq 0.01$; ###/*** $p \leq 0.001$.

cell culture, the addition of 1 μ M XAV reduced the relative volume of 5-FU-treated HCT116/FU spheroids by 7% ($P=0.006$) and had no significant effect on 5-FU treatment efficiency in HCT116 and HCT116/OXA spheroids (Fig. 2.7 C).

In 2D cell culture, the cytotoxic effects of 0.06 mM and 0.3 mM OxaPt were decreased by the addition of 15 μ M XAV: the efficiency of 0.06 mM OxaPt was reduced for 13% in HCT116 cells ($P=0.002$) and for 16% in HCT116/FU cells ($P=0.027$); the efficiency of 0.3 mM OxaPt was reduced for 18% in HCT116/OXA cells ($P=0.001$) (Fig. 2.7 D). Meanwhile in the 3D cell culture, the effects of 1 μ M XAV on OxaPt cytotoxicity were cell line dependent: the addition of XAV increased the volume of OxaPt-treated HCT116/FU spheroids by 11% ($P=0.002$); decreased the volume of OxaPt-treated HCT116/OXA spheroids by 16% ($P=0.001$); had no effect on the volume of OxaPt-treated HCT116 spheroids (Fig. 2.7 E).

2.4 Notch1 signaling

The activation of Notch1 signaling was evaluated by measuring the amounts of NOTCH1 intracellular domain (NICD1). In the 2D cell culture, untreated chemoresistant HCT116/FU and HCT116/OXA cells had increased amounts of NICD1: it was 2.2 folds higher in HCT116/FU cells ($P<0.001$) and 1.6 folds higher in HCT116/OXA cells ($P=0.009$) than in HCT116 cells (Fig. 2.8 A). In the 3D cell culture, the levels of this protein were 2.9 folds higher in HCT116/FU spheroids than in HCT116 spheroids ($P=0.003$). However, no statistically significant differences in the NICD1 levels were evident when untreated HCT116/OXA and HCT116 spheroids were compared.

The level of NICD1 in HCT116 cells grown in the 2D cell culture was only affected by the high doses of 5-FU and OxaPt: 0.3 mM 5-FU reduced NICD1 amount for 68% ($P<0.001$) and 0.06 mM OxaPt reduced it for 44% ($P<0.001$). The treatment with 5-FU or

OxaPt reduced NICD1 amount in HCT116/FU cells at all doses tested: 0.1 mM 5-FU for 34% ($P=0.004$), 0.3 mM 5-FU for 63% ($P<0.001$), 0.03 mM OxaPt for 53% ($P=0.001$), 0.06 mM OxaPt for 79% ($P<0.001$). In HCT116/OXA cells, the changes in NICD1 level were detected only after 5-FU treatment: 0.1 mM 5-FU decreased NICD1 amount for 31% ($P=0.027$) and 0.3 mM 5-FU for 65% ($P=0.002$), as compared to untreated HCT116/OXA cells.

The importance of Notch signaling for the cytotoxic effects of 5-FU and OxaPt were studied using γ -secretase inhibitor RO4929097 (RO). When used as a single treatment 5 μ M RO did not affect cell viability in the 2D cell culture (Fig. 2.3 C). However, 1 μ M RO was cytotoxic for chemoresistant HCT116/FU and HCT116/OXA spheroids: it reduced the relative volumes of HCT116/FU and HCT116/OXA spheroids by 25% ($P<0.001$) and 11% ($P=0.001$), respectively (Fig. 2.8 B, D). In the 2D cell culture, the cytotoxic effect of 5-FU was not affected by the addition of 5 or 10 μ M RO (data not shown). However, in the 3D cell culture, the addition of 1 μ M RO increased 5-FU cytotoxicity to chemoresistant spheroids: the relative volume of 5-FU-treated HCT116/FU spheroids was reduced by 6% ($P=0.017$), while the volume of 5-FU-treated HCT116/OXA spheroids was reduced by 28% ($P<0.001$) (Fig. 2.8 B). In the 2D cell culture, the cytotoxic effect of 0.06 mM OxaPt was decreased by the addition of 5 μ M RO: viability increased for 14% in HCT116 cells ($P=0.005$), for 24% in HCT116/FU cells ($P=0.007$) and 23% in HCT116/OXA cells ($P=0.003$) as compared to single OxaPt treatment (Fig. 2.3 C). In the 3D cell culture, the cytotoxic effect of OxaPt was also decreased by RO treatment: 1 μ M RO increased the relative volume of OxaPt-treated HCT116 spheroids by 29% ($P<0.001$), while the volumes of OxaPt-treated HCT116/FU and HCT116/OXA spheroids were increased a bit less – by 13% ($P=0.004$) and 16% ($P<0.001$), respectively (Fig. 2.8 D).

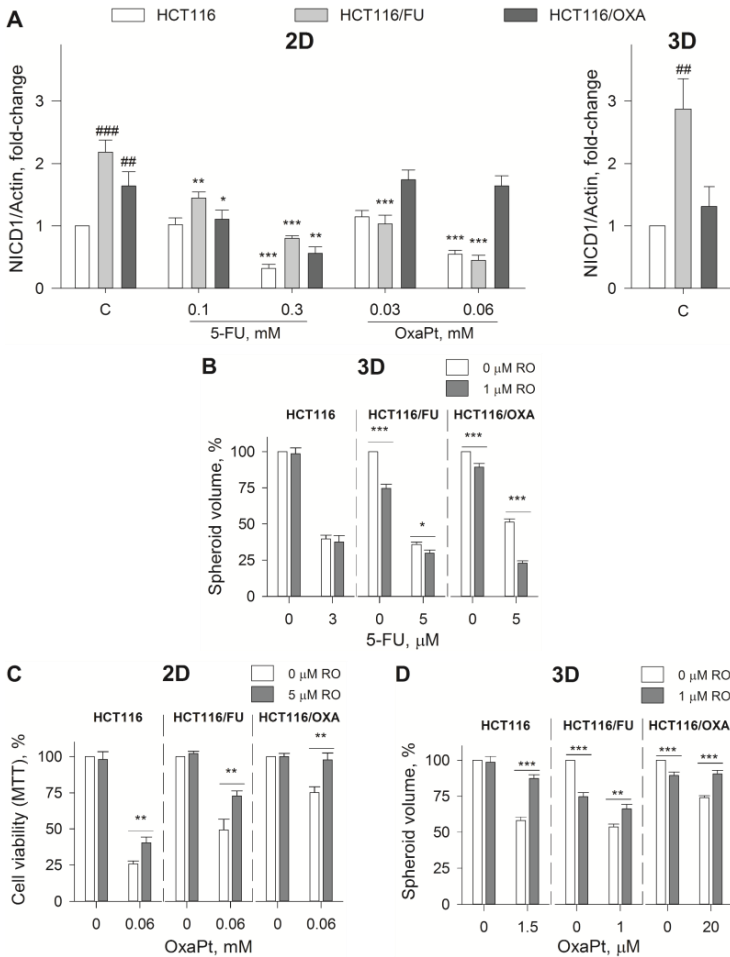


Fig. 2.8 The effects of 5-FU and OxaPt on Notch signaling. A, Western blot analysis of NICD1 at 48 h after exposure to drugs in monolayer cell culture (2D model) and in control spheroids at 168 h after initiation (3D model). The effects of RO on 5-FU cytotoxicity in the 3D (B) cell culture. The effects of RO on OxaPt cytotoxicity in the 2D (C) and 3D (D) cell culture. Cell viability was determined at 48 h after exposure to drugs using MTT assay. Relative spheroid volume was determined at 120 h after drug addition. C, untreated cells; n=3; Error bars \pm SD. #, a statistically significant difference between HCT116/FU or HCT116/OXA vs. HCT116 cells; *, a statistically significant difference between treated vs. control cells. * $p < 0.05$; ##/** $p \leq 0.01$; ###/*** $p \leq 0.001$.

2.5 Transcription repressor HES1

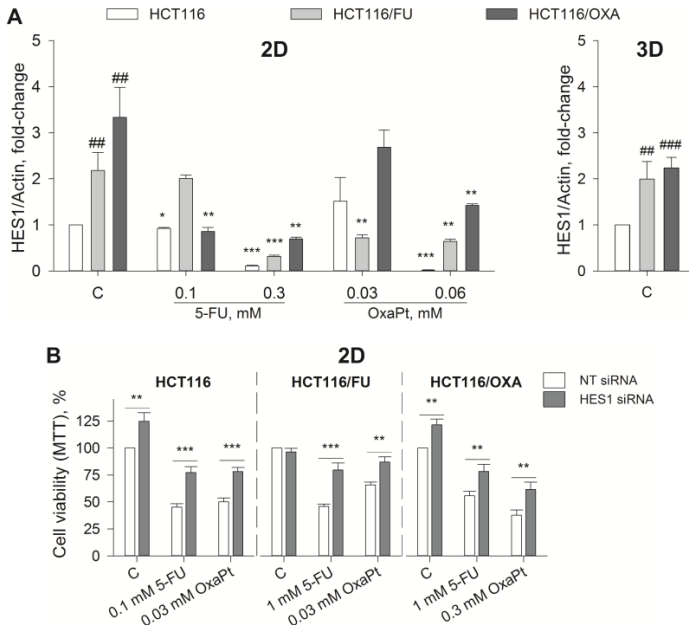


Fig. 2.9 HES1 protein level and effects of its silencing on 5-FU and OxaPt cytotoxicity. A, Western blot analysis of HES1 at 48 h after exposure to drugs in monolayer cell culture (2D model) and in control spheroids at 168 h after initiation (3D model). B, the effects of HES1 silencing on 5-FU and OxaPt cytotoxicity. HES1 was downregulated by transfection of HES1 targeting siRNA at 24 h prior to exposure to drugs. Cell viability was determined at 48 h after exposure to drugs using MTT assay. C, untreated cells; n=3; Error bars \pm SD.

#, a statistically significant difference between HCT116/FU or HCT116/OXA vs. HCT116 cells;

*, a statistically significant difference between treated vs. control cells.

* $p < 0.05$; ##/##* $p \leq 0.01$; ###/###* $p \leq 0.001$.

Even though transcription repressor HES1 was first identified as Notch target (Iso *et al.*, 2002), the expression of this protein is also affected by other signaling pathways such as Wnt, Hedgehog and TGF β (Borggreffe *et al.*, 2016). The level of HES1 protein in untreated chemoresistant cells/spheroids was significantly upregulated as compared to untreated HCT116 cells/spheroids: in HCT116/FU cells the increase was for 2.2 folds ($P=0.006$) and in

HCT116/FU spheroids – for 2 folds ($P=0.002$); in HCT116/OXA cells the increase was for 3.3 folds ($P=0.003$) and in HCT116/OXA spheroids – for 2.2 folds ($P<0.001$) (Fig. 2.9 A). The level of HES1 in HCT116 cells grown in the 2D cell culture was affected by both 5-FU doses and high dose of OxaPt: 0.1 mM 5-FU reduced HES1 level for 8% ($P=0.03$), 0.3 mM 5-FU reduced it for 89% ($P<0.001$), while at 0.06 mM dose HES1 was almost undetectable ($P<0.001$). High dose of 5-FU and both OxaPt doses reduced HES1 protein levels in HCT116/FU cells: after 0.3 mM 5-FU, it was reduced for 86% ($P=0.001$), after 0.03 mM OxaPt – for 67% ($P=0.003$) and after 0.06 mM OxaPt – for 71% ($P=0.002$). In HCT116/OXA cells HES1 protein levels were decreased by both 5-FU doses and high OxaPt dose: for 74% after 0.1 mM 5-FU ($P=0.003$), for 79% after 0.3 mM 5-FU ($P=0.002$) and for 57% after 0.06 mM OxaPt ($P = 0.007$), as compared to untreated control.

The impact of HES1 for the cytotoxic effects of 5-FU and OxaPt was tested by siRNA mediated downregulation of this protein levels. At 48 h post siRNA transfection, the reduction of HES1 protein levels in all cell lines was similar – it was reduced for approx. 45% (data not shown). Downregulation of HES1 increased the viability of HCT116 and HCT116/OXA cells by approx. 20% ($P=0.004$ for HCT116, $P<0.001$ for HCT116/OXA) and did not affect the viability of HCT116/FU cells (Fig. 2.9 B). When HES1-silenced cells were treated with 5-FU or OxaPt, cell viability was increased: the sensitivity of HCT116 cells for both treatments decreased for approx. 20% ($P<0.001$ for 5-FU and $P<0.001$ for OxaPt); the sensitivity of HCT116/FU cells for 5-FU treatment decreased for 34% ($P<0.001$) and for OxaPt treatment – for 20% ($P=0.002$); the sensitivity of HCT116/OXA cells for both treatments decreased for approx. 20% ($P=0.008$ for 5-FU and $P=0.008$ for OxaPt). The similar tendencies were seen when HES1 expression was downregulated for approx. 80% using ON-TARGETplus HES1 SMARTpool siRNA (data not shown).

3. Discussion

In this dissertation, the importance of autophagy and Wnt, Notch signaling pathways for the response of human colorectal cancer cell line HCT116 and its chemoresistant sublines HCT116/FU, HCT116/OXA to 5-FU or OxaPt treatment was investigated. In 2D and 3D cellular models, HCT116/FU exhibited increased resistance to 5-FU treatment, while HCT116/OXA cells were more resistant to both 5-FU and OxaPt treatments, as compared to HCT116 cells. Various molecular changes can lead to increased cell resistance to a certain drug. The resistance to 5-FU treatment is often caused by the increased drug efflux, the decreased expression of proteins involved in 5-FU metabolic activation or overexpression of thymidylate synthase, one of the main 5-FU targets (Longley and Johnston, 2005; Temraz *et al.*, 2014; Jensen *et al.*, 2012). Meanwhile, the acquired resistance to OxaPt is associated with increased nucleotide DNA excision repair and altered levels of antioxidants, glutathione or metallothioneins (Jensen *et al.*, 2012). Cells can also acquire the co-resistance to multiple drugs with different modes of action. Thus the comparison of molecular response patterns of cells featuring different type of resistance could help identify processes which are important for chemoresistance.

Our results revealed, that when compared to cells grown in the 2D model, HCT116/FU and HCT116/OXA spheroids were less resistant to 5-FU, whereas HCT116/OXA spheroids were more resistant to OxaPt. It was suggested that 5-FU could have higher cytotoxic effects in the 2D model because this drug targets only the proliferating cells, thus having less effect on the quiescent cells in spheroids (Tung *et al.*, 2011). Meanwhile, OxaPt can kill not only proliferating but also quiescent cells. Furthermore, hypoxia found in spheroids could increase cell resistance to OxaPt (Roberts *et al.*, 2009).

The growing amount of evidence suggests that photodynamic treatment could be used for overcoming the acquired chemoresistance of cancer cells (Spring *et al.*, 2015). In our study, we found that the sensitivity of HCT116 and HCT116/FU cells to mTHPC-PDT was similar. That means that HCT116/FU cells did not acquire cross-resistance to PDT, which is usually associated with increased expression of ABCG2 transporter (Liu *et al.*, 2007). It was previously shown that the cytotoxicity of mono-L-aspartyl chlorin e6 based PDT to 5-FU resistant or sensitive esophageal squamous cell carcinoma cells was also similar (Ohashi *et al.*, 2014). We have found that the combination of 5-FU and mTHPC-PDT inhibited the viability of the HCT116 cells with a significant effect both by 5-FU and PDT, but in the case of HCT116/FU cells, the added value of 5-FU in the combination of 5-FU and PDT was not significant. So the action of PDT, although efficient *per se*, does not eliminate the acquired restrictions in the cells imposed by chemoresistance. The additive effect of PDT and 5-FU was already reported in the case of glioblastoma multiforme (Christie *et al.*, 2017) and superficial esophageal squamous cell carcinoma (Kawazoe *et al.*, 2010).

In order to test the relevance of a specific process to cells chemoresistance, two strategies were chosen. First, the evaluation of this process activity was carried out. The activation of autophagy was measured by ATG7 protein, which is involved in the growth of autophagic membranes. The amounts of autophagosomes were estimated by measuring the levels of LC3B-II protein. The degradation of autophagosomes was determined by LC3B-II turnover in the presence and the absence of lysosomal degradation. The activation of canonical Wnt signaling was assessed by measuring the amounts of non-phosphorylated β -catenin at residues S33, S37, and T41 (the active form of β -catenin). The protein amounts of Notch1 intracellular domain (NICD1) was used as a reporter of Notch1 receptor activation. Furthermore, the levels of transcription repressor HES1, which can be affected by both Notch

and Wnt signaling (Borggrefe *et al.*, 2016), were also evaluated. Second, the impact of this signaling/process on cellular response to the effects of 5-FU or OxaPt was tested using small-molecule inhibitors or siRNA. Wnt/ β -catenin signaling was inhibited using tankyrase inhibitor XAV. Notch signaling was inhibited using γ -secretase inhibitor RO. HES1 or ATG7 levels were downregulated by specific siRNA.

We had determined that the amount of autophagosomes in HCT116/FU cells was higher, while in HCT116/OXA cells it was lower than in HCT116 cells (Table 3.1). The opposite trends were detected in different CRC cell lines – the 5-FU resistant SNUC5 cells had slightly lower (Yao *et al.*, 2017), while OxaPt resistant HT29 cells had the higher amount of autophagosomes than the parental cell lines (Sun *et al.*, 2017). The similar basal autophagic flux was detected in HCT116, HCT116/FU, HCT116/OXA cells, thus no significant changes were evident in the intensity of autophagosome degradation. The downregulation of ATG7 levels using siRNA revealed that autophagy had a negative effect on the proliferation of HCT116 and HCT116/FU cells. It has been demonstrated that autophagy can reduce the cell division rate by promoting dephosphorylation and degradation of c-Myc, which is facilitated by AMBRA1-dependent PP2A phosphatase (Cianfanelli *et al.*, 2015).

Our results uncovered that the activation of Wnt/ β -catenin signaling was increased in chemoresistant HCT116/FU and HCT116/OXA cells as compared to HCT116. The higher activation of Wnt/ β -catenin signaling in several 5-FU resistant CRC cell lines also have been documented (He *et al.*, 2018; Ayadi *et al.*, 2015). The XAV doses used in this study downregulated the protein levels of active β -catenin and HES1. That means that XAV decreased the activation of Wnt/ β -catenin signaling and this signaling at least partially regulated the levels of HES1. It is important to note, that in HCT116, HCT116/FU and HCT116/OXA cells, the heterozygous activating in-frame deletion of S45 in β -catenin was detected (the

unpublished data of A. Laurinavičius et al.). Thus a portion of cellular β -catenin could not be sent for degradation by the β -catenin destruction complex. Nevertheless, the stimulation of HCT116 cells with Wnt3A ligand leads to an increase in β -catenin protein levels and activation of TCF/LEF promoter (Wu *et al.*, 2012). We noticed that 15 μ M XAV was not cytotoxic to HCT116, HCT116/FU and HCT116/OXA cells grown in the 2D cell model, while 1 μ M XAV reduced the volume of HCT116/FU and HCT116/OXA spheroids. These XAV effects on HCT116 cells is supported by other studies where the targeted deletion of mutated β -catenin had no significant effect on HCT116 cell proliferation: cell doubling times in 2D cell model (Sekine *et al.*, 2002) and the rates of xenograft growth in the mouse model were not affected (Kim *et al.*, 2002). Our results suggest that the proliferation of chemoresistant HCT116/FU and HCT116/OXA cells in the 3D model might be more dependent on Wnt/ β -catenin signaling.

Table 3.1. The activation of Wnt/ β -catenin, Notch1 signaling pathways and autophagy extent in HCT116/FU and HCT116/OXA cells vs. HCT116 cells

| Protein | Model | Cell line | |
|-------------------------|-------|-----------|------------|
| | | HCT116/FU | HCT116/OXA |
| active β -catenin | 2D | ↑ | ↑ |
| | 3D | ↑ | ↑ |
| NICD1 | 2D | ↑ | ↑ |
| | 3D | ↑ | - |
| HES1 | 2D | ↑ | ↑ |
| | 3D | ↑ | ↑ |
| LC3B-II | 2D | ↑ | ↓ |
| ATG7 | 2D | ↑ | ↑ |

↑/↓, the relative increase/decrease in protein levels for ≥ 1.5 -folds;

↑/↓, the relative increase/decrease in protein levels which is statistically significant, but lower than 1.5-folds

We demonstrated that NICD1 protein level was higher in chemoresistant HCT116/FU (both in the 2D and 3D model) and HCT116/OXA cells (only in the 2D model) as compared to HCT116 cells. Other authors had reported the increased amount of Notch1

receptor in 5-FU resistant HCT8 cells and 5-FU or OxaPt resistant HCT116 cells (Dinicola *et al.*, 2016; Liu *et al.*, 2016; Huang *et al.*, 2015). The doses of γ -secretase inhibitor RO used in this study reduced the protein amounts of NICD1 and HES1, which indicates the downregulation of Notch signaling. RO was not cytotoxic for HCT116, HCT116/FU and HCT116/OXA cells grown in the 2D cell model, while in the 3D cell model decreased the volume of HCT116/FU and HCT116/OXA spheroids. That could imply that the proliferation of HCT116/FU and HCT116/OXA cells grown in 3D cell model might be more dependent on Notch signaling. Similar effects were reported in another study, where another γ -secretase inhibitor – DAPT was more potent to inhibit the growth of 5-FU or OxaPt resistant HCT116 cells xenographs (Huang *et al.*, 2015). It is possible that in HCT116/OXA spheroids another Notch receptor might be activated since these spheroids were more sensitive to Notch signaling inhibition, but NICD1 levels were similar to the levels found in HCT116 spheroids.

In our study, the chemoresistant HCT116/FU and HCT116/OXA cells had higher level of HES1 protein than HCT116 cells (both in the 2D and 3D model). Similar results in 2D model were already documented (Huang *et al.*, 2015). We determined that the proliferation of HCT116 and HCT116/OXA cells was increased after HES1 downregulation using siRNA. The increased cell proliferation after HES1 downregulation could be linked to the decreased cell sensitivity to contact-inhibition, which were previously described in preadipocytes (Noda *et al.*, 2011).

The 5-FU treatment had a negative effect on autophagy in HCT116 and HCT116/FU cells: it leads to the downregulation of ATG7 protein levels, decreased amounts of autophagosomes and inhibited autophagic flux (Table 3.2). In HCT116/OXA cells, 5-FU effect was slightly weaker: the amounts of autophagosomes were increased, while ATG7 levels and autophagic flux were decreased. It

Table 3.2. The effects of 5-FU or OxaPt on Wnt/ β -catenin, Notch1 signaling activity, and autophagy extent

| Cell line | Drug | Concentration | active β -catenin | NICD1 | HES1 | LC3B-II | Autophagic flux | ATG7 |
|-------------------|-------|---------------|-------------------------|-------|------|---------|-----------------|------|
| HCT116 | 5-FU | 0.1 mM | - | - | ↓ | ↓ | - | ↓ |
| | | 0.3 mM | ↓ | ↓ | ↓ | - | N | ↓ |
| | OxaPt | 0,03 mM | - | - | - | ↓ | ↑ | ↓ |
| | | 0,06 mM | ↓ | ↓ | ↓ | ↑ | - | ↓ |
| HCT116/FU | 5-FU | 0.1 mM | ↓ | ↓ | - | ↓ | N | ↓ |
| | | 0.3 mM | ↓ | ↓ | ↓ | ↓ | N | ↓ |
| | OxaPt | 0.03 mM | - | ↓ | ↓ | ↓ | ↑ | ↓ |
| | | 0.06 mM | ↓ | ↓ | ↓ | - | N | ↓ |
| HCT116/OXA | 5-FU | 0.1 mM | ↓ | ↓ | ↓ | - | ↓ | - |
| | | 0.3 mM | ↓ | ↓ | ↓ | ↑ | ↓ | ↓ |
| | OxaPt | 0.03 mM | - | - | - | ↑ | - | ↑ |
| | | 0.06 mM | - | - | ↓ | ↓ | ↑ | ↑ |

-, no statistically significant change;

↑/↓, the relative increase/decrease in protein levels which is ≥ 1.5 -folds;

↑/↓, the relative increase/decrease in protein levels which is statistically significant, but lower than 1.5-folds;

N, the autophagic flux is not statistically significant

is important to note the logical consequence that ATG7 protein downregulation correlated with a decrease of autophagic flux. Other authors reported ATG7 ability to promote autophagic flux (Pattison *et al.*, 2011). The downregulation of ATG7 levels using siRNA did not affect 5-FU cytotoxicity (Table 3.3). Our results are supported by other studies where 5-FU decreased the amounts of autophagosomes in SNUC5 cells (Yao *et al.*, 2017), while in HCT116 cells reduced autophagic flux and decreased protein levels of ATG7, p62, BECLIN1 by 5-FU treatment were reported (Akpınar *et al.*, 2016). However, 5-FU effect might be cell type dependent, it had the opposite effect on autophagosome amounts in CRC cells WiDR and Lovo92 (Bijnsdorp *et al.*, 2010).

The autophagy was enhanced by OxaPt. In HCT116 and HT116/FU cells, the decrease in autophagosome amounts and ATG7 protein levels at 48 h post exposure to OxaPt was detected and autophagic flux was evident. In HCT116/OXA cells, OxaPt treatment increased the levels of ATG7 protein, the amounts of autophagosomes and autophagic flux. Furthermore, siRNA mediated downregulation of ATG7 levels reduced the sensitivity of HCT116, HCT116/FU, HCT116/OXA cells to OxaPt treatment. It suggests, that autophagy is promoted by OxaPt treatment and might have a negative effect on cell survival. The increase of autophagosome amounts after OxaPt treatment was reported in HT116, SW480, SW620, HT29 and HT29/OXA cells (Liu *et al.*, 2015; Yang *et al.*, 2015; Sun *et al.*, 2017). However, the inhibition of autophagy using shATG5 or shATG7 had the opposite effect on OxaPt cytotoxicity in SW480 and SW620 cells (Yang *et al.*, 2015).

Autophagy had been identified as an early response to photodamage which can isolate and degrade photodamaged organelles. Furthermore, the cells with an increased autophagic process may have an enhanced ability to bypass phototoxicity (Kessel and Evans, 2016; Kessel, 2015). In this study, we found that mTHPC-PDT upregulated the amounts of autophagosomes in HCT116 and HCT116/FU cells, but autophagic flux was inhibited. It

is known that mTHPC can be accumulated in the membranes of lysosomes (Leung *et al.*, 2002) and lysosomes photodamage can inhibit autophagic flux (Kessel *et al.*, 2012). The investigation of mTHPC-PDT with 5-FU revealed some differences in the autophagic response of HCT116 and HCT116/FU cells. As compared to single mTHPC-PDT, the addition of 5-FU resulted in decreased amounts of autophagosomes and increased autophagic flux in HCT116 cells. While in HCT116/FU cells the effects were opposite. Lower amounts of autophagosomes and elevated autophagic flux indicates that autophagy is efficient in HCT116 cells: the autophagosomes are swiftly degraded.

The activation of Wnt/ β -catenin signaling was reduced by 5-FU treatment in HCT116, HCT116/FU and HCT116/OXA cells. This effect could be related to the 5-FU ability to promote the expression of APC in HCT116 and HT29 cells (Das *et al.*, 2014), which could lead to increased degradation of β -catenin (Tortelote *et al.*, 2017). It is important to note that the opposite effect of 5-FU on Wnt/ β -catenin signaling was described in HCT8 cells (He *et al.*, 2018). In this study, XAV increased the cytotoxic effects of 5-FU on HCT116, HCT116/FU and HCT116/OXA cells grown in 2D cell model and HCT116/FU spheroids. That suggests that Wnt/ β -catenin signaling could increase the CRC cell resistance to 5-FU treatment and promote cell survival. It was reported that XAV could increase the 5-FU induced apoptosis in CRC cells SW480 and SW620 (Wu *et al.*, 2016).

OxaPt treatment reduced the activation of Wnt/ β -catenin signaling in HCT116 and HCT116/FU cells, while no effect on this signaling in HCT116/OXA cells was registered. The OxaPt ability to reduce the expression of the β -catenin gene in HCT116 cells was already documented (Yang *et al.*, 2016). Our study revealed that in the 2D cell model, XAV decreased the cytotoxic effects of OxaPt for HCT116, HCT116/FU, HCT116/OXA cells. These results are supported by the study mentioned above where the upregulation of

β -catenin promoted OxaPt cytotoxicity on HCT116 cells (Yang *et al.*, 2016). We unveiled, that in the 3D cell model XAV affected the cytotoxicity of OxaPt for chemoresistant spheroids only: in HCT116/FU spheroids the cytotoxicity of this drug was decreased (the same effect as in the 2D cell model), while in HCT116/OXA spheroids – increased (the opposite effect than in the 2D cell model). That means that Wnt/ β -catenin signaling promotes OxaPt-induced HCT116/FU cell. We hypothesize that the effect of Wnt/ β -catenin signaling on HCT116/OXA cell death/survival could depend on oxygen availability. It is reported that hypoxia (which is present in 3D model) could induce the Wnt/ β -catenin dependent expression of ID2 protein in CRC cells, which has anti-apoptotic and growth promoting effects (Dong *et al.*, 2016).

In this study, the Notch1 signaling was also reduced by 5-FU treatment in HCT116, HCT116/FU, HCT116/OXA cells. The inhibition of Notch signaling by RO increased the 5-FU cytotoxic effects on HCT116/FU and HCT116/OXA spheroids. Still, no effect was evident in cells grown in the 2D model. It suggests that resistance of HCT116/FU and HCT116/OXA spheroids to 5-FU could be promoted by Notch signaling. The effects of 5-FU treatment on HES1 levels were even stronger, compared to the decrease of NICD1 or active β -catenin levels, although the pattern was similar. However, the downregulation of HES1 had the opposite effect on 5-FU cytotoxicity than RO or XAV treatment. We could hypothesize, that the deregulation of other Wnt and Notch signaling targets by XAV and RO might be responsible for 5-FU cytotoxicity promotion.

Our results revealed that OxaPt treatment reduced Notch1 signaling in HCT116 and HCT116/FU cells, while no effect on this signaling in HCT116/OXA cells was registered. However, the increase in NICD1 and HES1 protein levels by 2 μ M OxaPt treatment was reported in HCT116 and SW620 cells (Meng *et al.*, 2009). RO doses used in our study decreased the OxaPt cytotoxic

effects in all cell lines grown in 2D or 3D cell models. That suggests that Notch signaling promotes cell death after OxaPt treatment. Our results are supported by another study, where the same effect was seen using γ -secretase inhibitors MRK003, DAPT, GSI-XII, GSI-XX. Furthermore, the decreased OxaPt cytotoxicity was registered not only on HCT116 but also on CRC cells HT29, HCT15, SW480, Colo205 (Timme *et al.*, 2013). The results of HES1 downregulation using siRNA coincide with RO effects on cell viability of OxaPt-treated cells. It suggests that increased HES1 levels could have a negative effect on cell survival after OxaPt treatment.

Table 3.3. The effects of Wnt/ β -catenin, Notch signaling inhibitors, HES1 or ATG7 siRNA on 5-FU or OxaPt cytotoxicity

| Inhibitor or siRNA | Drug | Model | Cell line | | |
|--------------------|-------|-------|-----------|-----------|------------|
| | | | HCT116 | HCT116/FU | HCT116/OXA |
| XAV | C | 2D | - | - | - |
| | | 3D | - | T | T |
| | 5-FU | 2D | ↑ | ↑ | ↑ |
| | | 3D | - | ↑ | - |
| | OxaPt | 2D | ↓ | ↓ | ↓ |
| | | 3D | - | ↓ | ↑ |
| RO | C | 2D | - | - | - |
| | | 3D | - | T | T |
| | 5-FU | 2D | - | - | - |
| | | 3D | - | ↑ | ↑ |
| | OxaPt | 2D | ↓ | ↓ | ↓ |
| | | 3D | ↓ | ↓ | ↓ |
| HES1 siRNA | C | 2D | P | - | P |
| | 5-FU | 2D | ↓ | ↓ | ↓ |
| | OxaPt | 2D | ↓ | ↓ | ↓ |
| ATG7 siRNA | C | 2D | P | - | P |
| | 5-FU | 2D | - | - | - |
| | OxaPt | 2D | ↓ | ↓ | ↓ |

C, cells which were not treated with the drug;

-, did not change cell viability;

T, toxic to cells which were not treated with the drug;

P, promoted the proliferation of cells which were not treated with the drug;

↑/↓, increased/lowered drug cytotoxicity

To sum up, this study indicates that Wnt/ β -catenin and Notch signaling promotes CRC cells resistance to 5-FU, while HES1 protein, Notch signaling and autophagy promotes cell death after OxaPt treatment.

CONCLUSIONS

- Chemoresistant HCT116/5-FU cells are sensitive to mTHPC-PDT. mTHPC-PDT inhibits autophagic flux.

- In all tested cell lines, 5-FU diminishes the autophagic flux, while OxaPt increases it. The downregulation of ATG7 has no impact on 5-FU cytotoxicity and weakens the effects of OxaPt.

- 5-FU decreases the Wnt/ β -catenin and Notch1 signaling in all tested cell lines, while OxaPt – decreases it only in OxaPt-sensitive cells.

- In all tested cell lines, the inhibition of Notch signaling augments the resistance to OxaPt.

- Chemoresistant cell spheroids are more sensitive to Wnt/ β -catenin and Notch signaling inhibition than HCT116 cell spheroids.

- The inhibition of Wnt/ β -catenin and Notch signaling sensitizes chemoresistant cell spheroids to 5-FU.

- The expression of HES1 is higher in chemoresistant cells than in HCT116 cells. In all tested cells, HES1 protein levels are downregulated by 5-FU and OxaPt, while HES1 silencing increases cells resistance to these drugs.

REFERENCES

1. Ayadi M, Bouygues A, Ouaret D, Ferrand N, Chouaib S, Thiery JP, *et al.* Chronic chemotherapeutic stress promotes evolution of stemness and WNT/beta-catenin signaling in colorectal cancer cells: implications for clinical use of WNT-signaling inhibitors. *Oncotarget*. 2015;6(21):18518-33.
2. Akpinar B, Safarikova B, Laukova J, Debnath S, Vaculova AH, Zhivotovsky B, *et al.* Aberrant DR5 transport through disruption of lysosomal function suggests a novel mechanism for receptor activation. *Oncotarget*. 2016;7(36):58286-301.
3. Antonioli M, Di Rienzo M, Piacentini M, Fimia GM. Emerging Mechanisms in Initiating and Terminating Autophagy. *Trends in biochemical sciences*. 2017;42(1):28-41.
4. Bijnsdorp IV, Peters GJ, Temmink OH, Fukushima M, Kruyt FA. Differential activation of cell death and autophagy results in an increased cytotoxic potential for trifluorothymidine compared to 5-fluorouracil in colon cancer cells. *International journal of cancer*. 2010;126(10):2457-68.
5. Borggreffe T, Lauth M, Zwijsen A, Huylebroeck D, Oswald F, Giaimo BD. The Notch intracellular domain integrates signals from Wnt, Hedgehog, TGFbeta/BMP and hypoxia pathways. *Biochimica et biophysica acta*. 2016;1863(2):303-13.
6. Celli JP, Solban N, Liang A, Pereira SP, Hasan T. Verteporfin-based photodynamic therapy overcomes gemcitabine insensitivity in a panel of pancreatic cancer cell lines. *Lasers in surgery and medicine*. 2011;43(7):565-74.
7. Chen JY, Mak NK, Yow CM, Fung MC, Chiu LC, Leung WN, *et al.* The binding characteristics and intracellular localization of temoporfin (mTHPC) in myeloid leukemia cells: phototoxicity and mitochondrial damage. *Photochemistry and photobiology*. 2000;72(4):541-7.
8. Chen W, Wong C, Vosburgh E, Levine AJ, Foran DJ, Xu EY. High-throughput image analysis of tumor spheroids: a user-friendly software application to measure the size of spheroids automatically and accurately. *Journal of visualized experiments : JoVE*. 2014(89).
9. Christie C, Pomeroy A, Nair R, Berg K, Hirschberg H. Photodynamic therapy enhances the efficacy of gene-directed enzyme prodrug therapy. *Photodiagnosis and photodynamic therapy*. 2017;18:140-8.
10. Cianfanelli V, Fuoco C, Lorente M, Salazar M, Quondamatteo F, Gherardini PF, *et al.* AMBRA1 links autophagy to cell proliferation and tumorigenesis by promoting c-Myc dephosphorylation and degradation. *Nature cell biology*. 2015;17(1):20-30.
11. Cuyle PJ, Prenen H. Current and future biomarkers in the treatment of colorectal cancer. *Acta clinica Belgica*. 2017;72(2):103-15.
12. Dallas NA, Xia L, Fan F, Gray MJ, Gaur P, van Buren G, 2nd, *et al.* Chemoresistant colorectal cancer cells, the cancer stem cell phenotype, and increased sensitivity to insulin-like growth factor-I receptor inhibition. *Cancer research*. 2009;69(5):1951-7.

13. Das D, Preet R, Mohapatra P, Satapathy SR, Siddharth S, Tamir T, *et al.* 5-Fluorouracil mediated anti-cancer activity in colon cancer cells is through the induction of Adenomatous Polyposis Coli: Implication of the long-patch base excision repair pathway. *DNA repair.* 2014;24:15-25.
14. Dinicola S, Pasqualato A, Proietti S, Masiello MG, Palombo A, Coluccia P, *et al.* Paradoxical E-cadherin increase in 5FU-resistant colon cancer is unaffected during mesenchymal-epithelial reversion induced by gamma-secretase inhibition. *Life sciences.* 2016;145:174-83.
15. Dong HJ, Jang GB, Lee HY, Park SR, Kim JY, Nam JS, *et al.* The Wnt/beta-catenin signaling/Id2 cascade mediates the effects of hypoxia on the hierarchy of colorectal-cancer stem cells. *Scientific reports.* 2016;6:22966.
16. Ferlay J, Soerjomataram I, Dikshit R, Eser S, Mathers C, Rebelo M, *et al.* Cancer incidence and mortality worldwide: sources, methods and major patterns in GLOBOCAN 2012. *International journal of cancer.* 2015;136(5):E359-86.
17. Fodale V, Pierobon M, Liotta L, Petricoin E. Mechanism of cell adaptation: when and how do cancer cells develop chemoresistance? *Cancer journal.* 2011;17(2):89-95.
18. Friedrich J, Seidel C, Ebner R, Kunz-Schughart LA. Spheroid-based drug screen: considerations and practical approach. *Nature protocols.* 2009;4(3):309-24.
19. Galluzzi L, Baehrecke EH, Ballabio A, Boya P, Bravo-San Pedro JM, Cecconi F, *et al.* Molecular definitions of autophagy and related processes. *The EMBO journal.* 2017;36(13):1811-36.
20. Goler-Baron V, Assaraf YG. Overcoming multidrug resistance via photodestruction of ABCG2-rich extracellular vesicles sequestering photosensitive chemotherapeutics. *PLoS one.* 2012;7(4):e35487.
21. He L, Zhu H, Zhou S, Wu T, Wu H, Yang H, *et al.* Wnt pathway is involved in 5-FU drug resistance of colorectal cancer cells. *Experimental & molecular medicine.* 2018;50(8):101.
22. Holohan C, Van Schaeybroeck S, Longley DB, Johnston PG. Cancer drug resistance: an evolving paradigm. *Nature reviews Cancer.* 2013;13(10):714-26.
23. Huang R, Wang G, Song Y, Tang Q, You Q, Liu Z, *et al.* Colorectal cancer stem cell and chemoresistant colorectal cancer cell phenotypes and increased sensitivity to Notch pathway inhibitor. *Molecular medicine reports.* 2015;12(2):2417-24.
24. Huang SM, Mishina YM, Liu S, Cheung A, Stegmeier F, Michaud GA, *et al.* Tankyrase inhibition stabilizes axin and antagonizes Wnt signalling. *Nature.* 2009;461(7264):614-20.
25. Iso T, Chung G, Hamamori Y, Kedes L. HERP1 is a cell type-specific primary target of Notch. *The Journal of biological chemistry.* 2002;277(8):6598-607.
26. Yang C, Zhou Q, Li M, Tong X, Sun J, Qing Y, *et al.* Upregulation of CYP2S1 by oxaliplatin is associated with p53 status in colorectal cancer cell lines. *Scientific reports.* 2016;6:33078.
27. Yang HZ, Ma Y, Zhou Y, Xu LM, Chen XJ, Ding WB, *et al.* Autophagy contributes to the enrichment and survival of colorectal cancer stem cells under oxaliplatin treatment. *Cancer letters.* 2015;361(1):128-36.

28. Yao CW, Kang KA, Piao MJ, Ryu YS, Fernando P, Oh MC, *et al.* Reduced Autophagy in 5-Fluorouracil Resistant Colon Cancer Cells. *Biomolecules & therapeutics.* 2017;25(3):315-20.
29. Yu CH, Yu CC. Photodynamic therapy with 5-aminolevulinic acid (ALA) impairs tumor initiating and chemo-resistance property in head and neck cancer-derived cancer stem cells. *PLoS one.* 2014;9(1):e87129.
30. Jensen NF, Smith DH, Nygard SB, Romer MU, Nielsen KV, Brunner N. Predictive biomarkers with potential of converting conventional chemotherapy to targeted therapy in patients with metastatic colorectal cancer. *Scandinavian journal of gastroenterology.* 2012;47(3):340-55.
31. Kawazoe K, Isomoto H, Yamaguchi N, Inoue N, Uehara R, Matsushima K, *et al.* Effects of photodynamic therapy for superficial esophageal squamous cell carcinoma in vivo and in vitro. *Oncology letters.* 2010;1(5):877-82.
32. Kessel D. Autophagic death probed by photodynamic therapy. *Autophagy.* 2015;11(10):1941-3.
33. Kessel D, Evans CL. Promotion of Proapoptotic Signals by Lysosomal Photodamage: Mechanistic Aspects and Influence of Autophagy. *Photochemistry and photobiology.* 2016;92(4):620-3.
34. Kessel DH, Price M, Reiners JJ, Jr. ATG7 deficiency suppresses apoptosis and cell death induced by lysosomal photodamage. *Autophagy.* 2012;8(9):1333-41.
35. Kim JS, Crooks H, Foxworth A, Waldman T. Proof-of-principle: oncogenic beta-catenin is a valid molecular target for the development of pharmacological inhibitors. *Molecular cancer therapeutics.* 2002;1(14):1355-9.
36. Klionsky DJ, Abdelmohsen K, Abe A, Abedin MJ, Abeliovich H, Acevedo Arozena A, *et al.* Guidelines for the use and interpretation of assays for monitoring autophagy (3rd edition). *Autophagy.* 2016;12(1):1-222.
37. Kopan R, Ijagan MX. The canonical Notch signaling pathway: unfolding the activation mechanism. *Cell.* 2009;137(2):216-33.
38. Kulbacka J, Chwilkowska A, Bar J, Pola A, Banas T, Gamian A, *et al.* Oxidative alterations induced in vitro by the photodynamic reaction in doxorubicin-sensitive (LoVo) and -resistant (LoVoDX) colon adenocarcinoma cells. *Experimental biology and medicine.* 2010;235(1):98-110.
39. Leung WN, Sun X, Mak NK, Yow CM. Photodynamic effects of mTHPC on human colon adenocarcinoma cells: photocytotoxicity, subcellular localization and apoptosis. *Photochemistry and photobiology.* 2002;75(4):406-11.
40. Li L, Tang P, Li S, Qin X, Yang H, Wu C, *et al.* Notch signaling pathway networks in cancer metastasis: a new target for cancer therapy. *Medical oncology.* 2017;34(10):180.
41. The Lithuanian Cancer Registry [Website]. Vilnius: Nacional Cancer Institute; 2012 [atnaujinta 2018 03 27; cituota 2018 03 30]. Adresas: <http://www.nvi.lt/vezio-registras>.
42. Lippai M, Szatmari Z. Autophagy-from molecular mechanisms to clinical relevance. *Cell biology and toxicology.* 2017;33(2):145-68.
43. Liu H, Yin Y, Hu Y, Feng Y, Bian Z, Yao S, *et al.* miR-139-5p sensitizes colorectal cancer cells to 5-fluorouracil by targeting NOTCH-1. *Pathology, research and practice.* 2016;212(7):643-9.

44. Liu W, Baer MR, Bowman MJ, Pera P, Zheng X, Morgan J, *et al.* The tyrosine kinase inhibitor imatinib mesylate enhances the efficacy of photodynamic therapy by inhibiting ABCG2. *Clinical cancer research : an official journal of the American Association for Cancer Research.* 2007;13(8):2463-70.
45. Liu W, Zhang Z, Zhang Y, Chen X, Guo S, Lei Y, *et al.* HMGB1-mediated autophagy modulates sensitivity of colorectal cancer cells to oxaliplatin via MEK/ERK signaling pathway. *Cancer biology & therapy.* 2015;16(4):511-7.
46. Longley DB, Harkin DP, Johnston PG. 5-fluorouracil: mechanisms of action and clinical strategies. *Nature reviews Cancer.* 2003;3(5):330-8.
47. Longley DB, Johnston PG. Molecular mechanisms of drug resistance. *The Journal of pathology.* 2005;205(2):275-92.
48. Marchal S, Francois A, Dumas D, Guillemin F, Bezdetnaya L. Relationship between subcellular localisation of Foscan and caspase activation in photosensitised MCF-7 cells. *British journal of cancer.* 2007;96(6):944-51.
49. Meng RD, Shelton CC, Li YM, Qin LX, Notterman D, Paty PB, *et al.* gamma-Secretase inhibitors abrogate oxaliplatin-induced activation of the Notch-1 signaling pathway in colon cancer cells resulting in enhanced chemosensitivity. *Cancer research.* 2009;69(2):573-82.
50. Mercer TJ, Gubas A, Tooze SA. A molecular perspective of mammalian autophagosome biogenesis. *The Journal of biological chemistry.* 2018;293(15):5386-95.
51. Mizushima N, Yoshimori T. How to interpret LC3 immunoblotting. *Autophagy.* 2007;3(6):542-5.
52. Nakatogawa H. Two ubiquitin-like conjugation systems that mediate membrane formation during autophagy. *Essays in biochemistry.* 2013;55:39-50.
53. Noda N, Honma S, Ohmiya Y. Hes1 is required for contact inhibition of cell proliferation in 3T3-L1 preadipocytes. *Genes to cells : devoted to molecular & cellular mechanisms.* 2011;16(6):704-13.
54. Ohashi S, Kikuchi O, Tsurumaki M, Nakai Y, Kasai H, Horimatsu T, *et al.* Preclinical validation of talaporfin sodium-mediated photodynamic therapy for esophageal squamous cell carcinoma. *PloS one.* 2014;9(8):e103126.
55. Panczyk M. Pharmacogenetics research on chemotherapy resistance in colorectal cancer over the last 20 years. *World journal of gastroenterology.* 2014;20(29):9775-827.
56. Pandurangan AK, Divya T, Kumar K, Dineshbabu V, Velavan B, Sudhandiran G. Colorectal carcinogenesis: Insights into the cell death and signal transduction pathways: A review. *World journal of gastrointestinal oncology.* 2018;10(9):244-59.
57. Pattison JS, Osinska H, Robbins J. Atg7 induces basal autophagy and rescues autophagic deficiency in CryABR120G cardiomyocytes. *Circulation research.* 2011;109(2):151-60.
58. Punt CJ, Tol J. More is less -- combining targeted therapies in metastatic colorectal cancer. *Nature reviews Clinical oncology.* 2009;6(12):731-3.
59. Reardon JT, Vaisman A, Chaney SG, Sancar A. Efficient nucleotide excision repair of cisplatin, oxaliplatin, and Bis-aceto-amine-dichloro-

cyclohexylamine-platinum(IV) (JM216) platinum intrastrand DNA diadducts. *Cancer research*. 1999;59(16):3968-71.

60. Roberts DL, Williams KJ, Cowen RL, Barathova M, Eustace AJ, Brittain-Dissont S, *et al.* Contribution of HIF-1 and drug penetrance to oxaliplatin resistance in hypoxic colorectal cancer cells. *British journal of cancer*. 2009;101(8):1290-7.

61. Roy S, Majumdar AP. Signaling in colon cancer stem cells. *Journal of molecular signaling*. 2012;7(1):11.

62. Saif MW, Chu E. Biology of colorectal cancer. *Cancer journal*. 2010;16(3):196-201.

63. Sekine S, Shibata T, Sakamoto M, Hirohashi S. Target disruption of the mutant beta-catenin gene in colon cancer cell line HCT116: preservation of its malignant phenotype. *Oncogene*. 2002;21(38):5906-11.

64. Senge MO, Brandt JC. Temoporfin (Foscan(R), 5,10,15,20-tetra(m-hydroxyphenyl)chlorin)--a second-generation photosensitizer. *Photochemistry and photobiology*. 2011;87(6):1240-96.

65. Spring BQ, Rizvi I, Xu N, Hasan T. The role of photodynamic therapy in overcoming cancer drug resistance. *Photochemical & photobiological sciences : Official journal of the European Photochemistry Association and the European Society for Photobiology*. 2015;14(8):1476-91.

66. Sun C, Wang FJ, Zhang HG, Xu XZ, Jia RC, Yao L, *et al.* miR-34a mediates oxaliplatin resistance of colorectal cancer cells by inhibiting macroautophagy via transforming growth factor-beta/Smad4 pathway. *World journal of gastroenterology*. 2017;23(10):1816-27.

67. Teiten MH, Bezdetnaya L, Morliere P, Santus R, Guillemin F. Endoplasmic reticulum and Golgi apparatus are the preferential sites of Foscan localisation in cultured tumour cells. *British journal of cancer*. 2003;88(1):146-52.

68. Temraz S, Mukherji D, Alameddine R, Shamseddine A. Methods of overcoming treatment resistance in colorectal cancer. *Critical reviews in oncology/hematology*. 2014;89(2):217-30.

69. Timme CR, Gruidl M, Yeatman TJ. Gamma-secretase inhibition attenuates oxaliplatin-induced apoptosis through increased Mcl-1 and/or Bcl-xL in human colon cancer cells. *Apoptosis : an international journal on programmed cell death*. 2013;18(10):1163-74.

70. Tortelote GG, Reis RR, de Almeida Mendes F, Abreu JG. Complexity of the Wnt/betacatenin pathway: Searching for an activation model. *Cellular signalling*. 2017;40:30-43.

71. Tung YC, Hsiao AY, Allen SG, Torisawa YS, Ho M, Takayama S. High-throughput 3D spheroid culture and drug testing using a 384 hanging drop array. *The Analyst*. 2011;136(3):473-8.

72. van der Flier LG, Clevers H. Stem cells, self-renewal, and differentiation in the intestinal epithelium. *Annual review of physiology*. 2009;71:241-60.

73. Wu X, Luo F, Li J, Zhong X, Liu K. Tankyrase 1 inhibitor XAV939 increases chemosensitivity in colon cancer cell lines via inhibition of the Wnt signaling pathway. *International journal of oncology*. 2016;48(4):1333-40.

74. Wu ZQ, Brabletz T, Fearon E, Willis AL, Hu CY, Li XY, *et al.* Canonical Wnt suppressor, Axin2, promotes colon carcinoma oncogenic activity. *Proceedings*

of the National Academy of Sciences of the United States of America. 2012;109(28):11312-7.

75. Zaroni M, Piccinini F, Arienti C, Zamagni A, Santi S, Polico R, *et al.* 3D tumor spheroid models for in vitro therapeutic screening: a systematic approach to enhance the biological relevance of data obtained. *Scientific reports*. 2016;6:19103.

76. Zhan T, Rindtorff N, Boutros M. Wnt signaling in cancer. *Oncogene*. 2017;36(11):1461-73.

LIST OF PUBLICATIONS

Kukcinaviciute E, Sasnauskiene A, Dabkeviciene D, Kirvelienu V, Jonusienu V. Effect of mTHPC-mediated photodynamic therapy on 5-fluorouracil resistant human colorectal cancer cells. *Photochem Photobiol Sci.* 2017 Jul 1;16(7):1063-1070.

Kukcinaviciute E, Jonusienu V, Sasnauskienu A, Dabkevicienu D, Eidenaite E, Laurinavicius A. Significance of Notch and Wnt signaling for chemoresistance of colorectal cancer cells HCT116. *J Cell Biochem.* 2018 Jul;119(7):5913-5920.

CONFERENCE REPORTS

Kukcinaviciute E, Jonusienu V, Sasnauskienu A, Kirvelienu V. The effects of mTHPC-PDT to chemo-resistant human colorectal carcinoma cells HCT116. XIV International Conference of Lithuanian Biochemical Society, June 28-30, 2016, in Druskininkai, Lithuania.

Kukcinaviciute E, Jonusienu V, Sasnauskienu A, Kirvelienu V. The impact of mTHPC-PDT and 5-fluorouracil on autophagic flux in chemoresistant human colorectal carcinoma cells HCT116. *Life Sciences Baltics* 2016, September 14-15, 2016, Vilnius, Lithuania.

Kukcinaviciute E, Eidenaite E, Jonusienu V, Sasnauskienu A, Dabkevicienu D, Laurinavicius A. The role of Notch signaling for chemoresistance of colorectal cancer cells HCT116 in 2D and 3D culture models. *Cellular signaling and cancer therapy*, September 14-18, 2018, Cavtat, Croatia.

Zitkute V, **Kukcinaviciute E**, Dabkevicienu D, Jonusienu V, Starkuvienu V, Sasnauskienu A. The effects of 5-Fluorouracil and Oxaliplatin on Autophagy in Chemoresistant Colorectal Carcinoma Cells HCT116. *The Coins*, February 26-28, 2019, Vilnius, Lithuania.

CURRICULUM VITAE

Name Eglė

Surname Kukcinavičiūtė

Date of birth 1990-05-07

Address Vilnius University Life Sciences Center Institute of Biosciences
Saulėtekio 7, LT-10257, Vilnius, Lithuania
tel.: +37052234436
e-mail: egle.kukcinaviciute@gmail.com

Education

2014 – 2018 PhD student of Biochemistry, Vilnius University

2014 MSc of Biochemistry, Vilnius University

2012 BSc of Biochemistry, Vilnius University

Work experience

2012 september – 2019 february Specialist, Vilnius University, department of Biochemistry and Molecular Biology

2017 january – 2018 december Researcher, Vilnius University, department of Pathology, Forensic Medicine and Pharmacology

Research interests Cell biology and biochemistry

ACKNOWLEDGEMENTS

I would like to express my gratitude to all the people who have helped and motivated me throughout my PhD studies.

My supervisors – prof. dr. Vida Kirvelienė for the opportunity to work at the Laboratory of Cell Biochemistry and encouragement to improve my professional skills, dr. Aušra Sasnauskienė for her excellent guidance and support.

All my colleagues for help, interesting discussions, useful advices and great working atmosphere, especially dr. Daiva Dabkevičienė for assistance and lessons on biostatistics, dr. Violeta Jonušienė for assistance and advice with the preparation of publications, Vida Piskarskienė for taking care that we would always have everything that is needed for cell cultivation, Neringa Daugelavičienė for friendliness, Eigilė Eidėnaitė and Vilmantė Žitkutė for assistance in performing some experiments, their friendship and shared great time.

The ones who shared different laboratory facilities: prof. dr. Edita Sužiedelienė for permission to use NanoDrop, dr. Danutė Labeikytė – spectrophotometer, Aurimas Stulpinas – fluorimeter, the Department of Immunology and Cell Biology – microscope.

Prof. dr. Arvydas Laurinavičius for the possibility to work in the project.

Milda for the support and being there.

My parents, sister and Lukas for patience and unconditional belief in me.

NOTES

Vilniaus universiteto leidykla
Universiteto g. 1, LT-01513 Vilnius
El. p. info@leidykla.vu.lt,
www.leidykla.vu.lt
Tiražas 20 egz.